The Development of Improved
Blowout Prevention Systems
for
Offshore Drilling Operations
(Shallow Gas Hazards)

- A. T. Bourgoyne -
Louisiana State University

June 12, 1989

This report presents the status of research conducted by Louisiana State University on the design and operation of diverter systems. Further research is contemplated pending the results of an international workshop/symposium, to be sponsored by Minerals Management Service and the Petroleum Engineering Division of the U.K. Department of Energy. The Workshop is scheduled for November 28-29, 1989, in Baton Rouge, Louisiana.

FINAL REPORT
MMS Contract 14-12-0001-30274
June 12, 1989

# The Development of Improved Blowout Prevention Systems for Offshore Drilling Operations Part 1 – Shallow Gas Hazards

*by Adam T. Bourgoyne, Jr.*
*Louisiana State University*

## Introduction

In some marine environments, abnormal formation pressures may be encountered at very shallow depths, where conventional blowout prevention equipment and procedures are of no benefit. This can lead to very severe well control problems when permeable, gas bearing formations are penetrated. There have been numerous disasterous blowouts resulting from loss of well control after penetrating shallow, abnormally pressured gas formations. A research well facility at Louisiana State University has been used to study this problem under the sponsorship of the Minerals Management Service. A number of technical publications have resulted from this work. In this report, these technical contributions will be summarized and concepts used to minimize shallow gas hazards will be presented.

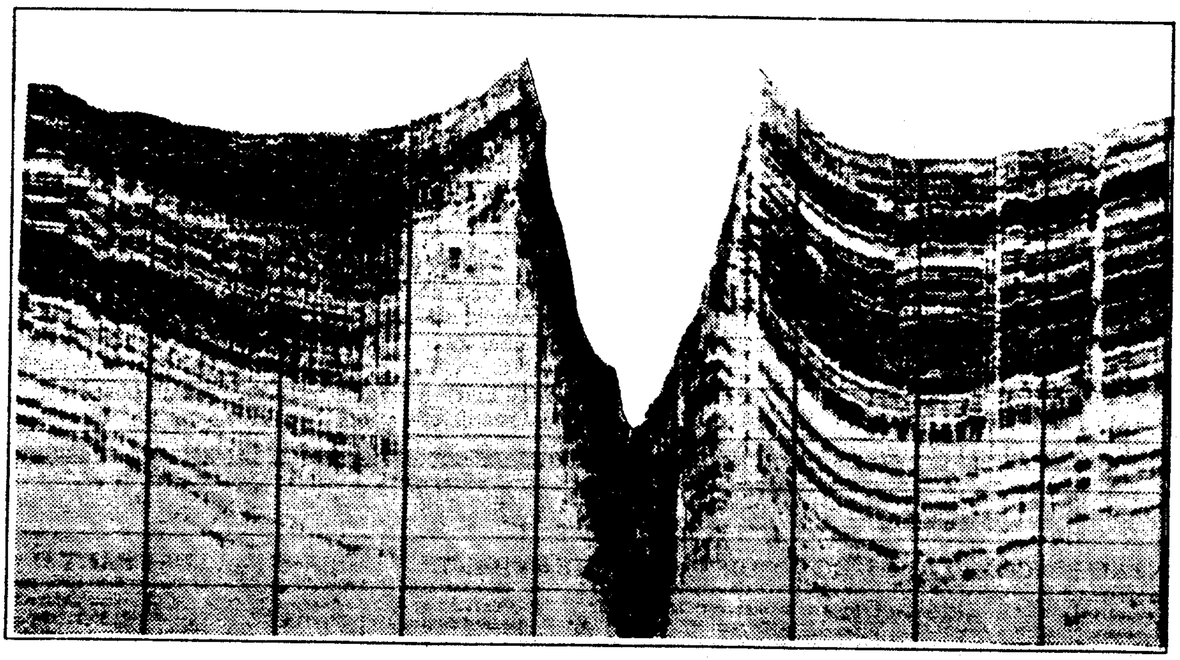

Figure 1. Side view of a crater on the sea floor thought to be due to a naturally occurring shallow gas blowout. (After Prior, Doyle, and Kaluza, 1989.) (Courtesy of Science Mag.)

Shallow gas accumulations are always at least slightly abnormally pressured in the upper portion of the reservoir due to the density difference between the gas in the reservoir and the water in the sediments surrounding the reservoir. Abnormal formation pore pressures that are approaching the formation fracture pressure are thought to be possible in sand lenses due to gas migration along fault planes from below. Shown in **Figure 1** is a recently discovered crater [**Prior, Doyle, and Kaluza, 1989**] in the floor of the Gulf of Mexico that is thought to be the result of a naturally occurring shallow gas blowout. It was discovered by a Shell Oil Company survey team in 2,176 meters (7,139 ft) of water, about 115 km ( 71 miles ) southeast of the Mississippi River delta. The crater was elliptical in shape, 58 m (190 ft) deep, 280 m (920 ft) across, and about 400 m (1300 ft) long. Slow seepage of the abnormally pressured gas was thought to be blocked by the formation of gas hydrates in the near surface sediments.

Even when the formation pore pressure is nearly normal, it is generally not feasible to shut-in a shallow gas flow when drilling from a bottom supported vessel. By the time the rig crew can recognize that the well has started to flow, the gas has already traveled a considerable distance up the open borehole. If the blowout preventers are closed, the pressure at the casing seat will generally build to a value exceeding the formation fracture pressure. If one or more fractures reach the surface, the resulting flow can destroy the foundations of a bottom-supported structure and ultimately lead to the formation of a crater. The rig shown in **Figure 2** eventually collapsed into a large crater in the seafloor.

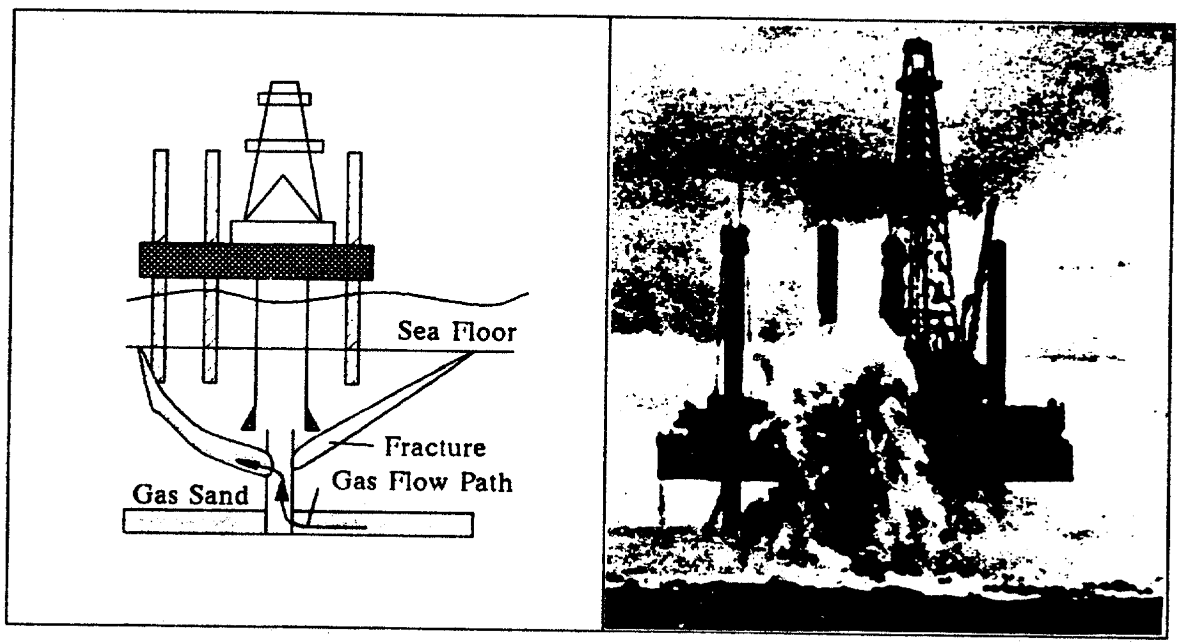


Figure 2 - Example blowout illustrating the need for a diverter system.

## Prevention of Shallow Gas Flows

Because of the difficulties in handling gas flows while drilling at shallow depths, considerable attention should be given to preventing such flows when planning the well and drilling the shallow portion of the well. Seismic surveys can sometimes be used to identify potential shallow gas zones prior to drilling (**Figure 3**). If localized gas concentrations are detected by seismic analysis, hazards can be reduced when selecting the surface well location.

When possible, empirical correlations should be applied to the seismic data to estimate formation pore pressures [**Bourgoyne et. al., 1986**]. This will sometimes permit the detection of shallow, abnormal pressure in the marine sediments. When formation pore pressures can be accurately estimated, an appropriate mud density program can be followed to prevent gas from entering the borehole.

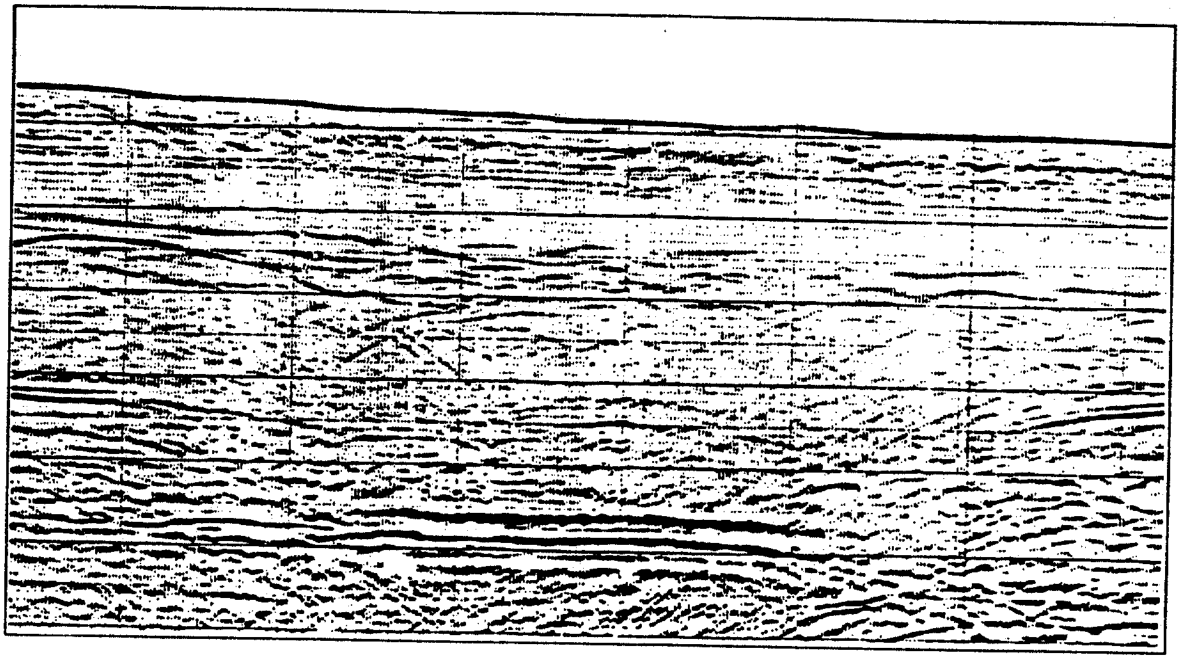

Figure 3. Example seismic profile showing possible shallow gas accumulation as darker reflection or "Bright Spot". (Courtesy of ARCO Oil and Gas).

Drilling practices followed when drilling the shallow portion of the well can also impact the blowout risk. Operations that can reduce downhole pressures, such as pulling the drill string from the well, should be carefully controlled to insure that a pressure overbalance is always maintained in the open borehole. Pressure changes due to pipe movement tend to increase with decreasing hole size, and thus would be more of a problem when drilling small diameter pilot holes. At shallow depths, a small loss in borehole pressure can result in a significant loss in equivalent mud density. For example, a pressure loss of 400 kPa (58 psi) when pulling pipe from a depth of 4,000 m (13,123 ft) is equivalent to a loss in drilling fluid density of only 10 $kg/m^3$ (0.08 lb/gal), which can be neglected. However, the same pressure loss of 400 kPa at only 400 m (1,312 ft) is equivalent to a loss in drilling fluid density of 102 $kg/m^3$ (0.85 lb/gal), which would be very dangerous. Trip–tank arrangements which keep the well completely full of drilling fluid at all times are better than those that require periodic refilling of the well. Modern top–drive rotary systems permit pumping down the drill–string while pulling pipe and can be used when necessary to eliminate the swabbing effect caused by pipe movement.

Gas–cut drilling fluid should also be watched very carefully when drilling the shallow portion of the well. When drilling at greater depths, even severe gas–cut mud observed at the surface generally will cause less than a 600 kPa (87 psi) reduction in bottom–hole pressure, which is usually within the allowable safety margin. Unfortunately, when drilling at very shallow depths, even the small pressure loss due to gas cut mud can be significant.

Conditions favoring a shallow gas flow due to gas–cut mud are most severe when drilling a large diameter hole at a high drilling rate with a long interval of open borehole. Drilled gas, which enters the drilling fluid from the sediments destroyed by the bit at the hole bottom may reduce the hydrostatic pressure opposite a more shallow sand below the allowable safety margin. This potential problem can be controlled by limiting the penetration rate of the bit. An approximate relationship between penetration rate and loss of borehole pressure was previously presented by **Bourgoyne, Hise, Holden and Sullins [1978]**. This relationship permits the development of guidelines for a maximum safe drilling rate in the shallow portion of the borehole. Shown in **Figure 4** are computed maximum safe drilling rates for a bit having a diameter of 0.4445 m (17.5 in.) cutting rock having a porosity of 28 % and a gas saturation of 85% when circulating a drilling fluid having a density of 1114 kg/m³ (9.3 lb/gal) at a rate of 5.30 $\times 10^{-2}$ m³/s (840 gal/min). The depth of the shallowest exposed gas sand that could flow, $D_1$, is 300 m (984 ft), and the pore pressure gradient was 10,500 Pa/m (0.465 psi/ft). Note that as the depth of the bit, $D_2$, increases, the maximum safe penetration rate decreases. Shown in **Figure 5** is a BASIC program that can be used to estimate the maximum safe drilling rate for other well conditions.

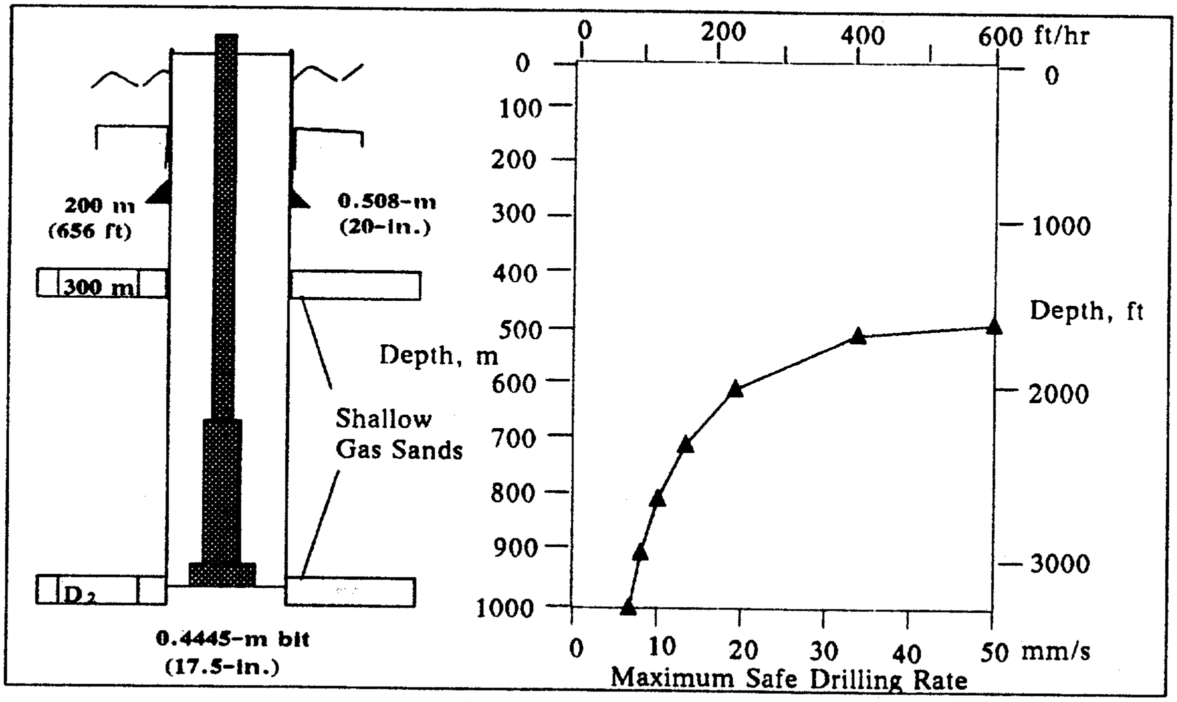


Figure 4 – Example calculation of maximum safe drilling rates when drilling multiple gas sands at shallow depths.

## Developing Contingency Plans

Unfortunately, use of existing technology does not always prevent the occurrence of shallow gas flows. Historical drilling records since 1965 for the Outer Continental Shelf of the Gulf of Mexico indicate that shallow gas flows have been encountered approximately on 1 well out of every 900 drilled. Shallow gas blowouts have accounted for 25 percent of all blowouts experienced in this area. In some other offshore development areas of the world, this percentage has been much higher. Thus, contingency plans must be developed to address this possibility.

Since 1975, a diverter system has been required for rigs drilling on the Outer Continental Shelf of the Gulf of Mexico. The function of the diverter system is to permit flow from the well to be directed overboard, away from the drilling personnel and rig structure. The essential elements of a diverter system includes:

(1) a vent line for conducting the flow away from the structure that is large enough to prevent a pressure build-up in the well to values above the fracture pressure,

(2) a means for closing the well annulus above the vent line during diverter operations, and

(3) a means for closing the vent line during normal drilling operations.

```
10 INPUT "Enter the pump flow rate in cubic meters/sec -             ", QM
20 INPUT "Enter the mud density in kg/cubic meters -                 ", RHO
30 INPUT "Enter the bit diameter in m          -                     ", D
40 INPUT "Enter the depth (d1) of the shallowest gas sand in m -     ", D1
50 INPUT "Enter the pore pressure gradient at d1 in Pa/m -           ", GP1
60 INPUT "Enter the depth of the bit (d2) in m -                     ", D2
70 INPUT "Enter the pore pressure gradient at d2 in Pa/m  -          ", GP2
80 INPUT "Enter the porosity at d2 as fraction -                     ", POR
85 INPUT "Enter the gas saturation at d2 as fraction -               ", SG
90 P1=GP1*D1+101300!
100 Z1 = 1! - 1.3E-08 * P1
110 QS = 0!
120 P2 = GP2 * D2 + 101300!
130 Z2 = 1! - 1.3E-08 * P2
140 X1 = 9.807 * RHO * D1 + 101300! - P1
150 XDEN = 8314*311 * Z1 * LOG( P1/101300! ) - 156.9 * D1
160 XNV  = X1 / XDEN
170 RP = 4!/3.14159* 8314*311 * XNV * Z2 * ( QM + QS )/( D^2 * POR * SG * P2 )
180 QS = 3.14159/4! * D^2 * RP * (1! - POR)
190 RHOA = (QS * 2.6 * 1000 + QM * RHO )/( QS + QM )
200 X2 = 9.807 * RHOA * D1 + 101300! - P1
210 IF  ABS(X2-X1) < 1  THEN GOTO 240 ELSE GOTO 220
220 X1 = X2
230 GOTO 150
240 PRINT "Density of Mud/Cuttings Mixture in kg/cubic meter = ",RHOA
250 PRINT "Maximum safe drilling rate in m/s  =                  ",RP
260 END
```

Figure 5 – Algorithm (BASIC programming language) for calculating maximum safe drilling rate at shallow depths in presence of drilled gas.

The sequence of events occurring when a shallow gas flow is encountered are illustrated in **Figure 6**. When the driller recognizes that the well has begun to flow, the diverter system is actuated (2b). This simultaneously causes the vent line to open and the annular diverter head to close. If the well plan calls for a dynamic well control method to be attempted with the rig pumps, the driller may continue to pump drilling fluid at the maximum possible rate as an attempt to regain control. As drilling fluid is displaced from the well, the rate of flow of gas into the well increases due to the loss in bottom-hole pressure (2c). After the well is unloaded of drilling fluid, a semi-steady-state condition is reached (2d) in which formation gas, water, and sand is flowing through the vent line. The loss of drilling fluid from the wellbore and the resulting decrease in pressure will usually result in an unstable borehole wall that will eventually cave-in and form a plug that stops the flow.

For many rigs, diverter systems have been added after rig construction, which have complicated the placement of vent lines. Also, since diverter systems are not routinely used, special testing and training is needed to insure maintenance of the diverter components and readiness of the rig crew to handle a shallow gas flow. Records available in the Events File of the Minerals Management Service indicate a diverter failure rate of approximately 50 percent during shallow gas flows.

The three most common modes of diverter failure have been:

(1) a failure of the vent line valve to open,

(2) formation fracture due to insufficient vent line size, and

(3) erosion.

Diverter design criteria have been developed that are directed at overcoming these common modes of diverter failure.

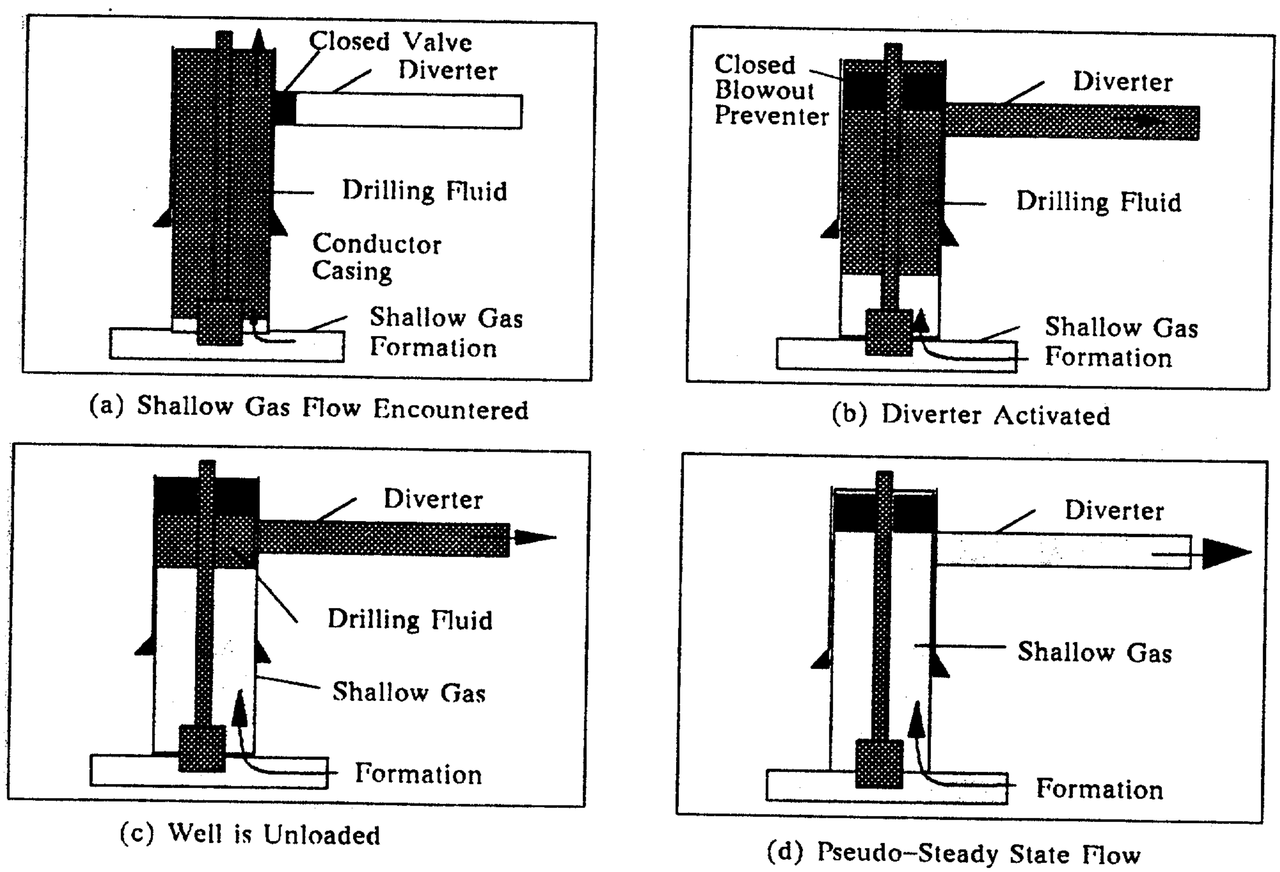


Figure 6 – Sequence of events modelled in experimental study of diverter operations.

## Diverter Design

In the past, diverter systems have been designed primarily based on surface pressure considerations. Equations for single phase flow of gas were used to select a vent line size that would result in a maximum acceptable wellhead pressure for a maximum anticipated gas flow rate. It was generally assumed in these calculations that the exit pressure of the diverter was atmospheric pressure. Many offshore rigs were equipped with 0.152–m (6–in.) diverter lines and until recently, this was considered acceptable practice by many offshore operators and by regulatory agencies. Experience with these systems in the Gulf of Mexico later provided evidence that larger diverter lines were sometimes needed.

An example incident that occurred on a Jack–up type rig in the Gulf of Mexico (offshore Texas) illustrates the need for a more complete analysis of diverter operating conditions. Two 0.152–m (6–in.) diverter lines were attached to 0.762–m (30–in.) casing, which was set at 149 m (490 ft), and penetrated 58 m (190 ft) of sediments. A 0.251–m (9.875–in.) pilot hole was drilled to 351 m (1150 ft). The well plan called for enlargement of the hole to 0.508–m (20–in.) prior to setting conductor casing. However, a gas flow was encountered after pulling two stands of the drill–string out of the hole. The diverter system was actuated and both diverter lines were opened. Both mud pumps were used to circulate fluid into the well as fast as possible in an attempt to regain control. The rig began to list slightly and was evacuated. Within the next 12 hours, the rig turned over and sank into a subsea crater which formed beneath the rig. The well stopped flowing after six days, and was thought to have bridged.

**Beck, Langlinais, and Bourgoyne [1987]** have suggested an improved diverter design procedure. They recommend that the final well design should consider the gas reservoir, borehole, casing, and diverter linked together as a single hydraulic system. A *systems analysis* approach [**Brown and Beggs, (1977), Crouch and Pack, (1980)** and **Clark and Perkins, (1980)**] permits the simultaneous calculation of pressures throughout the wellbore and diverter. Through this type of analysis, it can be determined if a successful diverter operation can be maintained using the design under consideration. The predicted operating pressures can be used to evaluate the working pressure of diverter components and the tendency for formation fracture at the casing seat. This approach can be used to determine the minimum safe conductor setting depth for expected well conditions and for the available diverter size. If a practical casing program cannot be achieved with the diverter available on the rig, then the benefits achieved by increasing the diverter size can be evaluated.

In performing the systems analysis, **Beck, Langlinais, and Bourgoyne [1986]** have shown that the flow at the diverter exit is usually sonic, and the assumption of atmospheric pressure at the diverter exit can lead to large errors. They also showed that near the diverter exit, a significant pressure gradient resulted from fluid acceleration, which could also cause significant errors if ignored. Experimental data was obtained in a model diverter system to permit evaluation of various methods for calculating flowing pressures for single and multiphase flow at near sonic conditions.

The systems analysis is accomplished by defining the pressure change occurring in each system component as a function of flow rate. The calculation is most easily accomplished by starting at the diverter exit, and proceeding stepwise through each component of the flow path to obtain the bottom–hole pressure. The calculation is repeated for several assumed exit pressures or flow rates to define a flow–string resistance curve. An inflow performance equation is used to model the flowing reservoir pressure at the borehole wall as a function of flow rate. The pseudo steady–state flow rate that will be observed during the diverter operations is determined from the intersection of the flow–string resistance curve and the formation–inflow performance curve.

*Exit Velocity Calculation*

The limiting (sonic) velocity at the diverter exit can be computed for any fluid using

$$v_e = \frac{1}{\sqrt{\rho\ c}} \tag{1}$$

where ρ is the density of the fluid and c is the compressibility of the fluid. For liquids, the density, ρ, and compressibility, c, can be assumed constant and are easily defined. For gases, the density can be determined from the real-gas equation, and is given by

$$\rho_g = \frac{p\ \bar{M}}{z\,R\,T} \tag{2}$$

for any given pressure, p, gas molecular weight, M, gas deviation factor, z, and temperature, T, at the diverter exit. The coefficient ,R, is the universal gas constant for the system of units being used. For most accurate results, the gas compressibility should be computed assuming a polytropic process. This assumption gives

$$c_g = \frac{1}{n\,p} \tag{3}$$

where n is the polytropic expansion coefficient for the process. For an adiabatic expansion of an ideal gas, n becomes equal to the ratio, *k*, of specific heat at constant pressure, $C_p$, to specific heat at constant volume, $C_v$. For sonic flow through a restriction, *k* is often used as an approximate value for n.

When the fluid being produced from the well is a multiphase mixture, **Eqn. 1** can still be applied through use of appropriate values for effective density and effective compressibility. The effective multiphase density, $\rho_e$, can be calculated using

$$\rho_e = \lambda_g\,\rho_g + \lambda_l\,\rho_l + \lambda_s\,\rho_s \tag{4}$$

where λ denotes the volume fraction (hold-up) and subscripts g, l, and s denotes the gas, liquid, and solid phases present. For sonic flow, the slip velocity between the phases can be neglected when calculating the volume fractions, λ. **Wallis [1969]** recommended calculating an effective compressibility, $c_e$, in a similar manner using

$$c_e = \lambda_g\,c_g + \lambda_l\,c_l + \lambda_s\,c_s \tag{5}$$

**Ross [1960]** had previously used this approach but for simplicity, considered the second and third terms of this equation to be negligible. Ross also suggested that *k* be determined for multiphase mixtures using

$$k_e = \frac{C_{pe}}{C_{ve}} = \frac{\chi_g C_p + \chi_l C_l + \chi_s C_s}{\chi_g C_v + \chi_l C_l + \chi_s C_s} \qquad (6)$$

where $\chi$ is the weight fraction (quality) of gas in the mixture, $C_p$ and $C_v$ are the heat capacities of the gas at constant pressure and constant volume respectively, $C_l$ is the heat capacity of the liquid phase, and $C_s$ is the heat capacity of the solid phase. **Wallis [1969]** did not adopt this method for determining the gas expansion coefficient, but instead used a constant value.

**Beck, Langlinais, and Bourgoyne [1987]** performed experiments in model diverter systems to measure sonic exit velocities for a natural gas having a specific gravity of 0.64. Data were presented for single and multiphase flow for diverter diameters of 0.0233–m (0.918–in.), 0.0492–m (1.937–in.), and 0.1244–m (4.897–in.). These data were used to determine experimental values for the polytropic expansion coefficient, n. Their results have been curve fitted and are shown in **Figure 7**. Note that the measured value of n varied with diverter diameter and gas weight percent (quality) for the range of conditions studied and could be approximately defined by

$$n = 2.8\, d^{0.25} \left[ 1 + 5.5 d^{0.5} ( 1 - \chi_g )^2 \right] \qquad (7)$$

where the diameter, d, is expressed in meters. The experimentally determined value of n departed significantly from $k$, especially for the largest diameter studied.

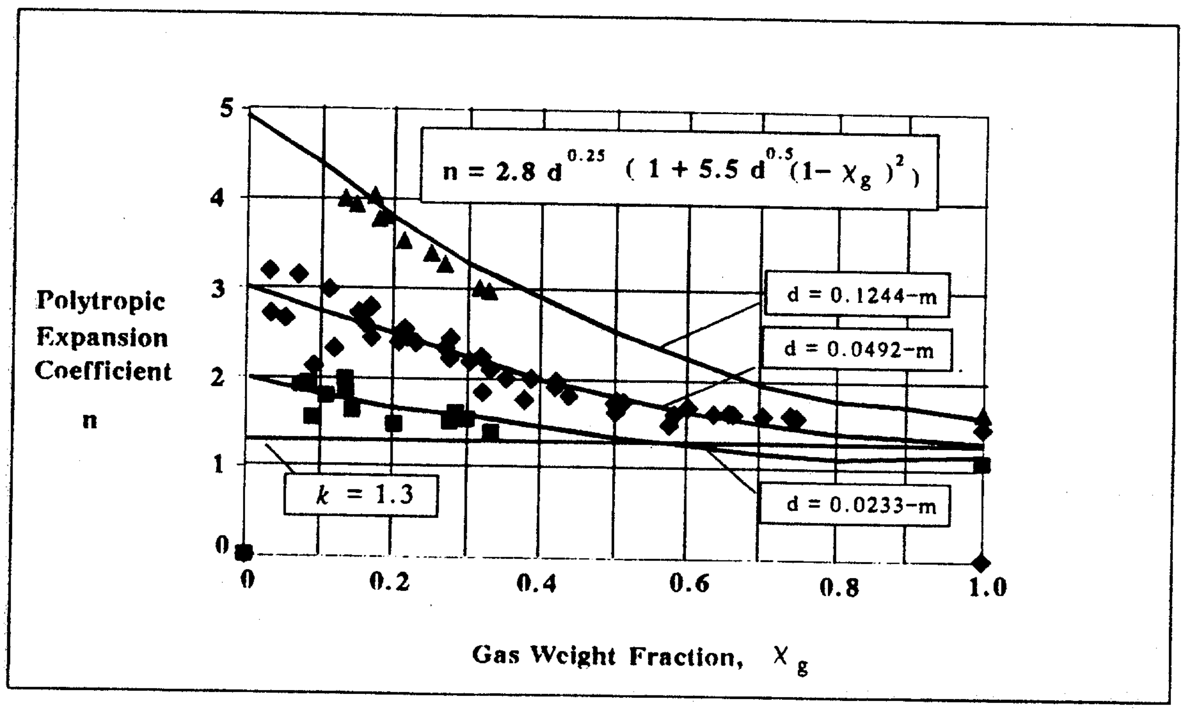


Figure 7 – Values of polytropic expansion coefficient, n, measured during experimental study of diverter operations.

The use of **Eqns. 1 - 5**, and **Eqn. 7** for calculating the relationship between flow rate and diverter exit pressure is illustrated in **Table 1** for a natural gas having a specific gravity of 0.64. It was assumed that no water was produced with the gas and thus the gas weight fraction (quality), $\lambda_g$, was 1.0. The temperature was assumed to be 38 °C (100 °F). The calculation was done for a 0.152-m (6-in.) diverter diameter that was previously the minimum size approved by the U.S Minerals Management Service and for a 0.254-m (10-in.) diverter diameter which is now required by this agency.

The calculation results given in **Table 1** show that a 0.254-m (10-in.) diverter diameter will handle approximately three times the flow rate of a 0.152-m (6-in.) diverter for a given exit pressure. For the smaller line, note that approximately 10 atmosphere of backpressure would result at the diverter exit for a design gas-flow rate of 83 $m^3/s$ ( 250 MMScf/D ).

Table 1

Example Calculation of Pressure-Flow Rate Relationship

0.152-m (6-in.) Diverter Exit

| (1) Pressure (Pa) | (psi) | (2) Gas Density Eqn.7.2 ($kg/m^3$) | (3) n Eqn.7.7 | (4) $c_g$ Eqn.7.3 ($Pa^{-1}$) | (5) Gas Volume Fraction $\lambda$ | (6) $V_e$ Eqn. 7.1 (m/s) | (7) Flow Rate at S.C. ($m^3/s$) | (MMScf/D) |
|---|---|---|---|---|---|---|---|---|
| 101,300 | 14.7 | 0.728 | 1.75 | $5.65 \times 10^{-6}$ | 0.999 | 493.2 | 8.34 | 25.4 |
| 200,000 | 29.0 | 1.441 | 1.75 | $2.86 \times 10^{-6}$ | 0.999 | 492.7 | 16.48 | 50.3 |
| 300,000 | 43.5 | 2.167 | 1.75 | $1.91 \times 10^{-6}$ | 0.999 | 492.2 | 24.75 | 75.5 |
| 400,000 | 48.0 | 2.896 | 1.75 | $1.43 \times 10^{-6}$ | 0.999 | 491.6 | 33.05 | 100.8 |
| 500,000 | 72.5 | 3.629 | 1.75 | $1.14 \times 10^{-6}$ | 0.999 | 491.1 | 41.37 | 126.2 |
| 1,000,000 | 145.0 | 7.345 | 1.75 | $5.72 \times 10^{-6}$ | 0.999 | 488.5 | 83.29 | 254.1 |

0.254-m (10-in.) Diverter Exit

| (1) Pressure (Pa) | (psi) | (2) Gas Density Eqn.7.2 ($kg/m^3$) | (3) n Eqn.7.7 | (4) $c_g$ Eqn.7.3 ($Pa^{-1}$) | (5) Gas Volume Fraction $\lambda$ | (6) $V_e$ Eqn. 7.1 (m/s) | (7) Flow Rate at S.C. ($m^3/s$) | (MMScf/D) |
|---|---|---|---|---|---|---|---|---|
| 101,300 | 14.7 | 0.728 | 1.99 | $4.97 \times 10^{-6}$ | 0.999 | 525.9 | 24.8 | 75.7 |
| 200,000 | 29.0 | 1.441 | 1.99 | $2.51 \times 10^{-6}$ | 0.999 | 525.3 | 49.1 | 149.7 |
| 300,000 | 43.5 | 2.167 | 1.99 | $1.68 \times 10^{-6}$ | 0.999 | 524.8 | 73.7 | 224.9 |
| 400,000 | 48.0 | 2.896 | 1.99 | $1.26 \times 10^{-6}$ | 0.999 | 524.2 | 98.4 | 300.2 |
| 500,000 | 72.5 | 3.629 | 1.99 | $1.01 \times 10^{-6}$ | 0.999 | 523.7 | 123.2 | 375.8 |
| 1,000,000 | 145.0 | 7.345 | 1.99 | $5.02 \times 10^{-6}$ | 0.999 | 520.8 | 248.0 | 756.7 |

*Flowing Pressure Gradient Calculation*

Upstream of the diverter exit, the pressure gradient, $\frac{dp}{dL}$, is given by the expression

$$\frac{dp}{dL} = \frac{\rho\, g \cos(\theta) + \dfrac{f \rho \bar{v}^2}{2\, d}}{1 - \rho \bar{v} \dfrac{dv}{dp}} \qquad (8)$$

where the first term of the numerator accounts for hydrostatic pressure changes and the second term accounts for frictional pressure losses. The term $\rho\ v\ dv$ in the denominator accounts for pressure changes caused by fluid acceleration. In the first term, g represents the acceleration of gravity, and $\theta$ represents the vertical deviation angle of the flow section under consideration. The Moody **[1944]** friction factor, $f$, in the second term is given by

$$\frac{1}{\sqrt{f}} = -2 \log_{10}\left(0.27\frac{\epsilon}{d} + \frac{2.52}{N_{Re}\sqrt{f}}\right) \qquad (9)$$

where $\epsilon$ is the absolute roughness. A value of 2 μm (0.000079–in.) for roughness was found to yield good agreement with experimental data. The Reynolds number, $N_{Re}$, is defined by

$$N_{Re} = \frac{\rho\, \bar{v}\, d}{\mu} \qquad (10).$$

In the denominator, the effect of fluid acceleration between any points 1 and 2 in a section of uniform area was found to be most accurately determined assuming a polytropic expansion model. Use of this model yields

$$\rho\ \bar{v}\ \frac{dv}{dp} = \frac{\bar{\rho}\ \bar{v}^2\ \bar{p}\ (p_1^{1/n} - p_2^{1/n})}{(p_2 - p_1)\ p_1^{1/n}\ p_2^{1/n}} \qquad (11).$$

At a sudden decrease in the area of the flow path, such as at the diverter entrance and at the bit, the pressure drop due to fluid acceleration can be estimated using

$$\Delta p_a = \rho \frac{\Delta v^2}{2} \qquad (12).$$

At a sudden increase in the area of the flow path, such as at the casing seat and at the top of the drill collars, the pressure increase due to fluid deceleration is generally small and can be neglected. Since there is no diffuser present that can provide a smooth transition to the larger flow area, almost all of the theoretical pressure recovery predicted by **Eqn 12** is lost to turbulence.

When the fluid being produced from the well is a multiphase mixture, **Eqns. 8 – 12** can be applied through use of appropriate values for effective density, effective viscosity, and effective velocity. For high flow rates typical of shallow gas flows, the effective multiphase density, $\rho_e$, viscosity, $\mu_e$, and velocity, $v_e$, can be calculated assuming no slippage between the phases. Thus, the effective multiphase density, $\rho_e$, is given by **Eqn. 4** and effective multiphase viscosity, $\mu_e$, is given by

$$\mu_e = \lambda_g \mu_g + \lambda_{ls} \mu_{ls} \tag{13}$$

where the subscript 'ls' refers to a liquid-solid slurry mixture and thus includes the effect of any solids present by including them in the liquid phase. The effective multiphase velocity, $v_e$, is defined in terms of flow rate, q, and cross sectional area, A, by

$$v_e = \frac{q_g + q_l + q_s}{A} \tag{14}$$

The use of **Eqns. 8 – 14** for calculating the flowing pressure gradients upstream of the diverter exit is illustrated in **Table 2** for the same conditions used in the calculation of **Table 1** and a diverter length of 30 m (98 ft). The other well conditions correspond to the example diverter failure discussed previously for the jackup rig that was lost offshore Texas. The 0.762-m (30-in.) casing that was set at 149 m (490 ft) was assumed to have a 0.0254-m (1-in.) wall thickness. The drill string was composed of 224 m (735 ft) of drillpipe having an outer diameter of 0.127-m (5-in.) and 100 m (328 ft) of drill collars having an outer diameter of 0.191-m (7.5-in.). Beneath the bit was 27 m (89 ft) of open borehole having a diameter of 0.251-m (9.875-in.). The projected area of the bit that partially blocked the annular flow path was equivalent to a diameter of 0.222-m (8.74-in.). The starting point of the calculation was a gas flow rate of 33.05 $m^3/s$ (100.8 MMScf/D), which corresponds to the fourth entry in **Table 1**. For this flow rate, the calculated absolute pressure at the gas formation was 2,823,300 Pa (410 psi). By repeating this calculation for a number of different assumed gas flow rates, a flow-string resistance curve can be defined. Shown in **Figure 8** are flow-string resistance curves obtained in this manner for both a 0.152-m (6-in.) and a 0.254-m (10-in.) diverter diameter. Point D corresponds to the example calculation of **Table 2**.

When the shallow gas contingency plan calls for using two diverter lines of equal diameter in parallel, half of the total flow will exit through each of the diverter lines. This is easily handled in the analysis procedure illustrated above by using half of the total gas flow rate in the calculations of **Table 1** and in the surface diverter section of **Table 2**, and the total gas flow rate for the annulus and borehole sections of **Table 2**.

*Formation Productivity*

Resistance to flow is present in the gas reservoir as well as in the flow path to the surface. Since little is generally known about the properties of the gas reservoir causing the unexpected flow, detailed reservoir simulations are not usually justified. However, it is important to take into account turbulence and other factors that become important at high-gas velocities. The Forchheimer **[1901]** equation as adapted for radial, semi-steady state flow in a homogeneous gas reservoir is recommended for use in diverter design calculations. This equation can be arranged to give flowing bottom-hole pressure, $p_{bh}$, within a wellbore of radius, $r_w$, due to flow within a circular reservoir of external radius, $r_e$, and effective thickness, h, and having an average reservoir pressure, $p_r$. The Forchheimer equation for these conditions is defined by

$$p_{bh}^2 = \bar{p}_r^2 - \left[\frac{\mu \bar{T} \bar{z} p_{sc}}{\pi T_{sc} k h} \ln\left(0.472 \frac{r_e}{r_w}\right)\right] q_{sc} - \left[\frac{\beta \bar{z} M \bar{T} p_{sc}^2}{2 R \pi^2 T_{sc}^2 h^2}\left(\frac{1}{r_w} - \frac{1}{r_e}\right)\right] q_{sc}^2 \qquad (15)$$

where the subscript 'sc' denotes standard conditions. The terms in brackets reduce to a constant for a given reservoir. The second term is needed to properly model high–

Table 2

Example calculation of flow–path pressure drop

Flow rate assumed is 33.05 $m^3$ /s (100.8 MMScf/D) (Fourth entry in Table 7.I)
0.152–m (6–in.) Diverter attached to 0.762–m (30–in.) casing set at 149–m (490ft) with 0.251–m (9.875–in.) borehole at 351 m (1150 ft).

| (1) Pressure (Pa) | (psi) | (2) Pressure Step | (3) Mean Pressure | (4) Gas Density Eqn.7.2 (kg/m³) | (5) Gas Velocity (m/s) | (6) Pressure Gradient Eqn.7.8 (Pa /m) | (7) Length Step (m) | (8) Total Length (m) | (9) Total Depth (m) |
|---|---|---|---|---|---|---|---|---|---|
| Surface Diverter, d = 0.152m, θ = 90, n = 1.75, $\mu = 1\times10^{-5}$ Pa.s, $N_{Re} = 2.16\times10^{7}$, f = 0.01225 | | | | | | | | | |
| 400,000 | 48.0 | 50,000 | 425,000 | 3.079 | 462.4 | 237,200 | 0.211 | | |
| 450,000 | 65.3 | 100,000 | 500,000 | 3.629 | 392.4 | 63,100 | 1.584 | 0.21 | 0.00 |
| 550,000 | 79.8 | 100,000 | 600,000 | 4.365 | 326.2 | 33,700 | 2.967 | 1.80 | 0.00 |
| 650,000 | 94.3 | 100,000 | 700,000 | 5.104 | 278.9 | 23,700 | 4.215 | 4.76 | 0.00 |
| 750,000 | 108.8 | 100,000 | 800,000 | 5.848 | 243.5 | 18,600 | 5.381 | 8.98 | 0.00 |
| 850,000 | 123.3 | 100,000 | 900,000 | 6.595 | 215.9 | 15,400 | 6.494 | 14.36 | 0.00 |
| 950,000 | 137.8 | 119,000 | 1,009,500 | 7.417 | 192.0 | 13,000 | 9.129 | 20.85 | 0.00 |
| 1,069,000 | 155.0 | Acceleration Pressure Drop at Diverter Entrance = 136,600 Pa | | | | | | 29.98 | 0.00 |
| 1,205,600 | | | | | | | | 29.98 | 0.00 |
| Casing–drillpipe annulus, $d_2$= 0.711m, $d_1$ =0.127m, θ = 0, n = 2.56, $\mu = 1\times10^{-5}$ Pa.s, $N_{Re} = 3.93\times10^{6}$, f = 0.01059 | | | | | | | | | |
| 1,205,600 | 174.9 | 13,800 | 1,212,500 | 8.953 | 7.5 | 92 | 149.0 | 29.98 | 0.00 |
| 1,219,400 | 176.9 | | | | | | | 179.0 | 149.0 |
| Borehole–drillpipe annulus, $d_2$= 0.251m, $d_1$ =0.127m, θ = 0, n = 1.91, $\mu = 1\times10^{-5}$ Pa.s, $N_{Re} = 8.70\times10^{6}$, f = 0.01283 | | | | | | | | | |
| 1,219,400 | 176.9 | 100,000 | 1,269,400 | 9.386 | 74.8 | 2,868 | 34.865 | 179.0 | 149.0 |
| 1,319,400 | 191.4 | 106,400 | 1,372,600 | 10.174 | 69.0 | 2,652 | 40.115 | 213.9 | 183.9 |
| 1,425,800 | 206.8 | | | | | | | 254.0 | 224.0 |
| Borehole–drillcollar annulus, $d_2$= 0.251m, $d_1$ =0.191m θ = 0, n = 1.78, $\mu = 1\times10^{-5}$ Pa.s, $N_{Re} = 7.45\times10^{6}$, f = 0.01475 | | | | | | | | | |
| 1,425,800 | 206.8 | 200,000 | 1,525,800 | 11.353 | 108.5 | 17,247 | 11.596 | 154.0 | 149.0 |
| 1,625,800 | 235.8 | 200,000 | 1,725,800 | 12.905 | 95.4 | 15,029 | 13.308 | 265.6 | 235.6 |
| 1,825,800 | 264.8 | 200,000 | 1,925,800 | 14.472 | 85.1 | 13,325 | 15.010 | 278.9 | 248.9 |
| 2,025,800 | 293.8 | 200,000 | 2,125,800 | 16.055 | 76.7 | 11,972 | 16.706 | 293.9 | 264.0 |
| 2,225,800 | 322.8 | 200,000 | 2,325,800 | 17.654 | 69.8 | 10,871 | 18.398 | 310.6 | 280.7 |
| 2,425,800 | 351.8 | 246,000 | 2,548,800 | 19.456 | 63.3 | 9,863 | 24.943 | 329.0 | 299.1 |
| 2,671,800 | 387.5 | Acceleration Pressure Drop past Bit = 138,100 Pa | | | | | | 354.0 | 324.0 |
| 2,809,900 | 407.5 | | | | | | | 354.0 | 324.0 |
| Borehole below bit, d = 0.251m, θ = 0, n = 1.98, $\mu = 1\times10^{-5}$ Pa.s, $N_{Re} = 1.37\times10^{7}$, f = 0.01128 | | | | | | | | | |
| 2,809,900 | 407.5 | 13,400 | 2,816,600 | 21.648 | 24.1 | 496 | 27.010 | 354.0 | 324.0 |
| 2,823,300 | 409.5 | | | | | | | 381.0 | 351.0 |

velocity gas flow where the velocity coefficient, β, is determined emperically. Note that once the bracketed terms are reduced to a constant, a relatively simple relationship between gas flow rate and flowing bottom-hole pressure results.

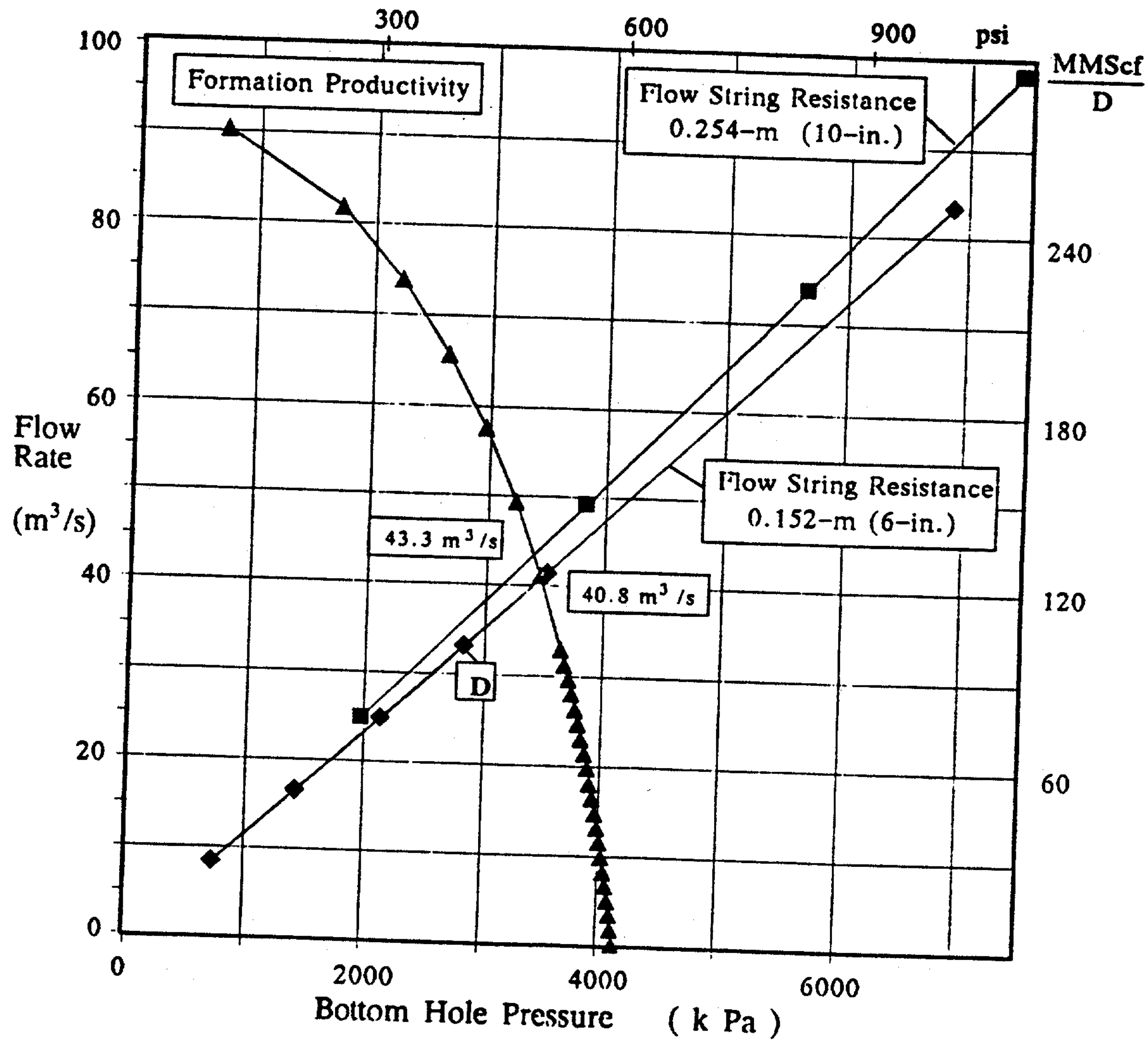


Figure 8 – Pseudo-steady-state systems analysis plot for example of Tables 1 and 2.

Laboratory core data shows that the velocity coefficient, β, tend to decrease with increasing permeability. Since shallow sands tend to be unconsolidated, a correlation based on data taken in unconsolidated samples [Johnson and Taliaferro, 1938] is recommended for diverter design calculations. The recommended correlation gives β in $m^{-1}$ using

$$\beta = \frac{1.031}{\sqrt{k}} \tag{16}$$

where the permeability, k, is given in $m^2$.

Choosing a representative value for the reservoir thickness, h, is complicated by the fact that the wellbore often penetrates through only part of the gas reservoir before the shallow gas flow is detected and drilling is stopped. When this is true, the gas flow is not truly radial as assumed by **Eqn. 15**, and an effective thickness value must be used. This effective thickness depends on the ratio of the horizontal to vertical permeability, the wellbore radius, $r_w$, the total formation thickness, $h_f$, and the formation thickness penetrated by the bit, $h_p$. When the vertical permeability is much less than the horizontal permeability, the effective thickness is approximately equal to the thickness penetrated by the bit. As the vertical permeability increases and approaches the horizontal permeability, the following equation presented by **Craft and Hawkins [1959]** can be used:

$$h = h_p \left[ 1 + 7 \sqrt{\frac{r_w}{2 h_p}} \cos\left( \frac{\pi}{2} \frac{h_p}{h_f} \right) \right] \qquad (17).$$

Shown in **Figure 8** is a formation producitivity curve that is representative of the example shallow gas reservoir encountered at a depth of 351m (1150 ft). The reservoir was assumed to have a permeability of 9.9 $\mu m^2$ (10,000 md), an effective thickness of 3.05 m (10 ft), an external radius of 305 m (1000 ft), and an average absolute reservoir pressure of 4,137,000 Pa (600 psi). Since well control was lost when pulling pipe from the borehole, it is possible that the entire reservoir thickness was penetrated by the bit. Shallow gas formations having a thickness of 3 m or less are difficult to detect using seismic data. The gas properties used were as previously defined for the calculations of **Tables 1** and **2**.

*Equilibrium Gas Flow Rate*

The equilibrium flow rate that will be observed during diverter operations is obtained from the intersection of the flow–string resistance curve and the formation–inflow performance curve. Note that for the example under consideration (**Figure 8**), the gas flow rate predicted is 40.8 $m^3/s$ (124 MMScf/D) for a 0.152–m (6–in.) diverter system and 43.3 $m^3/s$ (132 MMScf/D) for a 0.254–m (10–in.) diverter system.

Once the pseudo–steady–state gas flow rate has been determined, the pressure at various key points in the flow path can be established. This can be done by interpolation from the pressure traverses previously calculated in **Tables 1** and **2**, or by a new pressure traverse calculated for the equilibrium gas flow rate. It is important that the pressures in the open borehole are maintained below formation fracture pressure after pseudo–steady state conditions are reached. If borehole pressures are sustained above the formation fracture pressure for a long period of time, the probability that fracturing will reach the seafloor (**Figure 2**) is greatly increased.

*Formation Fracture Pressure*

**Constant and Bourgoyne [1989]** have recommended fracture pressure equations for offshore drilling operations based on Eaton's correlation. The recommended method gives the absolute overburden stress, $\sigma_{ob}$, in SI units in terms of the seawater depth, $D_{sw}$, and the sediment depth below the seafloor, $D_s$, using

$$\sigma_{ob} = 101{,}300 + 10{,}000\, D_{sw} + 25{,}500\, D_s - 21{,}980{,}000 \left[ 1 - \exp(-0.000279\, D_s) \right] \qquad (18).$$

The minimum expected absolute formation fracture pressure, $p_f$, is then determined from the absolute formation pore pressure, $p_p$, and the overburden pressure, $\sigma_{ob}$, by

$$P_f = P_p + \left[ 1 - 0.629 \exp(-0.00042\ D_s) \right] \left[ \sigma_{ob} - P_p \right] \qquad (19).$$

This minimum fracture pressure would correspond to extending an existing fracture in a sandy formation. Higher formation fracture pressures would be expected for fracture initiation and in plastic "gumbo" shale formations. The maximum expected pressure for fracture extension is the overburden pressure given by **Eqn 18**.

Table 3

Comparison of equilibrium pressure traverses for 0.152-m (6-in.) and 0.254-m (10-in.) diverter systems.

Water depth of 58 m and air gap of 33 m.

| Location | Depth (m) | (ft) | Pressure for 0.152-m system (Pa) | (psi) | Pressure for 0.254-m system (Pa) | (psi) | Minimum Fracture Extension Pressure (Pa) | (psi) |
|---|---|---|---|---|---|---|---|---|
| Diverter Exit | 0 | 0 | 494,000 | 72 | 176,500 | 26 | Protected by casing | |
| Wellhead | 0 | 0 | 1,485,000 | 215 | 488,000 | 71 | Protected by casing | |
| Casing Seat | 149 | 490 | 1,502,000 | 218 | 496,000 | 72 | 1,467,000 | 214 |
| | 174 | 571 | 1,602,000 | 232 | 799,800 | 116 | 1,846,000 | 270 |
| Top of drill collars | 224 | 735 | 1,755,000 | 255 | 1,116,500 | 162 | 2,692,000 | 394 |
| Bottom of drill collars | 324 | 1063 | 3,280,000 | 476 | 3,176,500 | 461 | 4,264,000 | 629 |
| Below bit | 324 | 1064 | 3,449,000 | 500 | 3,375,000 | 489 | 4,264,000 | 629 |
| Hole bottom | 351 | 1150 | 3,465,000 | 503 | 3,392,000 | 492 | 4,825,000 | 712 |

Shown in **Table 3** is a comparison of the borehole pressures and fracture pressures for the two diverter sizes considered in the example. Note that for the 0.152-m (6-in.) diverter system, the expected fracture pressure at the casing seat would be exceeded, whereas for the 0.254-m (10-in.) diverter system, a 971,000 Pa (141 psi) safety margin would exist.

*Working Pressure of Diverter Components*

The systems analysis procedure provides information about the pressures that could be expected on the diverter components after the well is unloaded and pseudo-steady-state conditions are reached. However, while the drilling fluid is being displaced from the well, the mud in the system behaves as a viscous plug which greatly slows the flow through the diverter. This results in a pressure peak occurring when the leading edge of the gas reaches the diverter entrance. The magnitude of the pressure peak depends primarily on the formation pressure and on the amount of mud that remains in the well due to slippage past the gas while the well is unloading. The pressure peak can be substancially higher than the equilibrium wellhead pressure calculated from a systems analysis procedure. This pressure peak is of short duration, typically lasting only a few seconds. If fracturing occures, it is unlikely that fracture propagation would move very far from the wellbore before the pressure subsides to the equilibrium value. As long as the equilibrium borehole pressure is less than the fracture extension pressure, there ia a high probability that the fracture will not propagate to the surface. Thus, it is recommended that the design load at the casing seat is based on equilibrium flowing conditions. However, the design load for surface diverter components should be based on the pressure peak occurring when the drilling fluid is being displaced from the well.

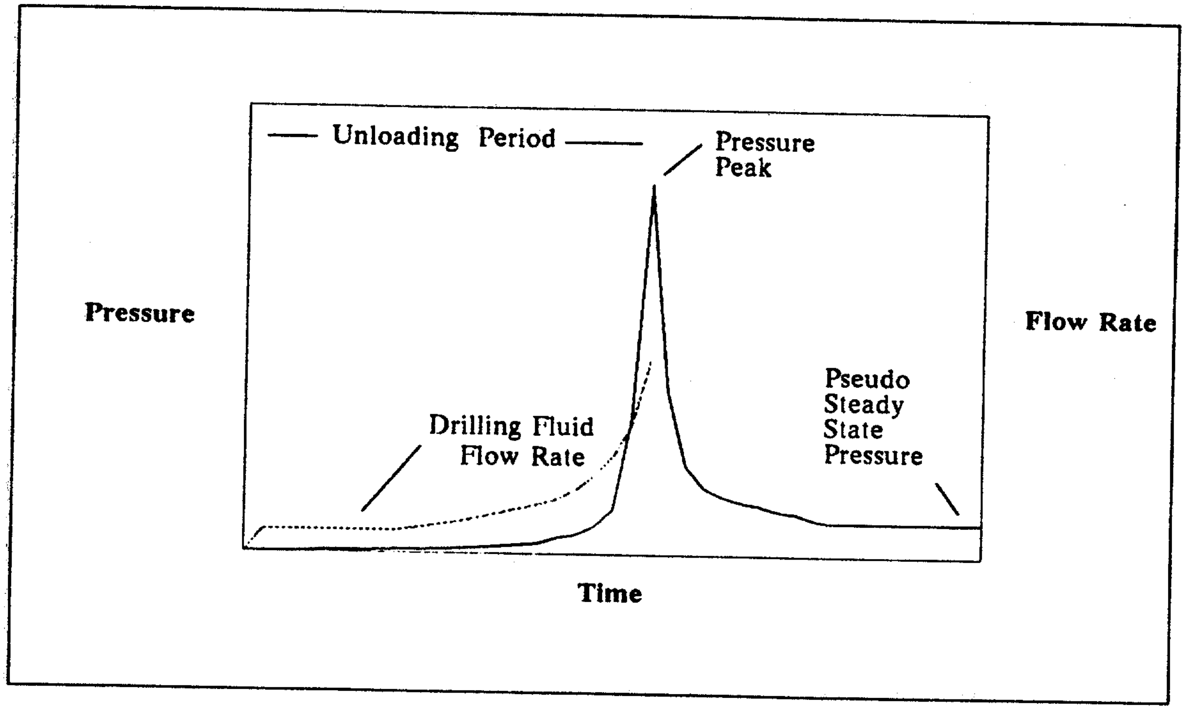


Figure 9 – Calculated pressure behavior Typical pressure and drilling fluid flow rate history observed during experimental study of diverter operations. ( After Santos, 1989. )

**Santos [1989]** performed experiments on a 0.152–m (6–in.) diverter system attached to a 382 m (1252 ft) well containing 0.178–m (7–in.) casing to study unsteady–state pressure behavior when the well is first placed on a diverter. In the experiments, the gas entering the bottom of the well flowed through a valve that was controlled by a process control computer that simulated the behavior of a formation. A program was developed for the flow control computer to permit a range of formation productivities to be simulated. Pressures were monitored during the experiments at a number of locations in the well and diverter. Experimental runs were made using a number of different mud systems.

Typical experimental results obtained by **Santos [1989]** for the pressure history and flow–rate history at any given point in the surface system during the simulated diverter operations are shown in **Figure 9**. Note that the flow rate from the well begins slowly but accelerates very quickly as gas approaches the surface. As the length of drilling fluid in the well decreases, the pressure imposed on the gas decreases, causing rapid expansion of the gas in the well and an increase in the gas flow rate into the bottom to the well. Note also the pressure peak in the diverter that is seen just before the bottom of the drilling fluid column exits the system. Eventually, a pseudo-steady-state condition is reached in which the pressures change very slowly with time due to reservoir depletion.

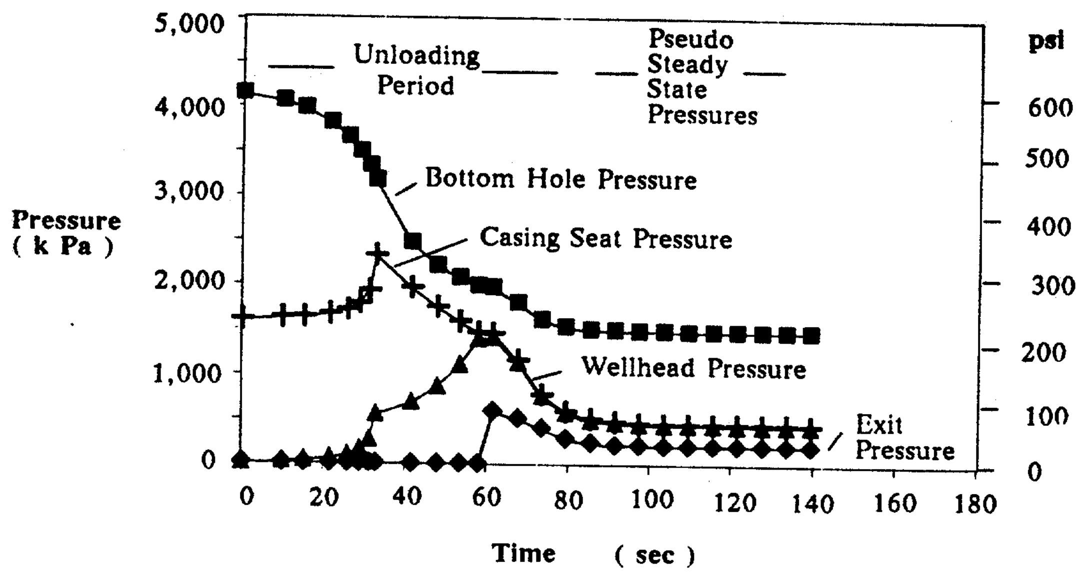


Figure 10 – Typical pressure and drilling fluid flow rate history observed during experimental study of diverter operations. ( After Santos, 1989. )

**Santos [1989]** developed a computer model for predicting the pressures and flow rates observed during a shallow gas flow as a function of both time and position. The program was first verified using the experimental results obtained with the model diverter system. The computed results for peak wellhead pressure matched the observed pressure peaks within an error band of about 25 percent. The program was then used to simulate a wide variety of field conditions. It was found that the peak wellhead pressure tended to decrease with decreasing formation pressure, decreasing formation productivity, and increasing diverter diameter. For the field conditions studied, the peak wellhead pressure was generally less than 65 percent of the formation pressure. Also, the time required to unload the well was typically only a few minutes.

Shown in **Figure 10** are results obtained using the computer model for the 0.254-m (10-in.) diverter system discussed in the previous example calculations. The drilling fluid in the well when the shallow gas flow began was assumed to have a density of 1116 kg/m$^3$ (9.3 lb/gal). Note that it is predicted that the well will unload in about one minute with a peak wellhead pressure of 1,436,000 Pa (208 psi), which was about 34 percent of the formation pressure. Thus a working pressure for diverter components of at least this value would be needed. The calculated pressure at the casing seat exceeds the minimum fracture extension pressure of 1,467,000 Pa (214 psi) during most of the first minute but drops to about 496,000 Pa (72 psi) after pseudo-steady state conditions are reached. Similar simulations performed for a 0.152-m (6-in.) diverter system gave a peak wellhead pressure of 2,620,000 Pa (380 psi), which was about 63 percent of the formation pressure.

*Diverter Anchors*

Some diverter failures have involved the anchor system used to hold the diverter piping in place. The anchor system should be carefully designed to withstand the forces resulting from the moving fluids. The maximum forces on the anchoring system occurs when the wellhead pressure reaches its peak value. When telescoping segments or slip joints are used below the annular blowout preventer, a maximum upward force on the wellhead must be resisted that is equal to the peak pressure multiplied by the internal annular cross sectional area at the slip joint. In computer simulations made by **Santos [1989]**, these forces sometimes reached as high as 1,300,000 N (300,000 lbf) for the field conditions studied. Similarly, a maximum axial thrust distributed along the length of the diverter exists which is equal to the peak pressure multiplied by the internal cross sectional area of the diverter. In addition, at bends in the diverter system, the anchor system must resist a force equal to the mass rate of flow multiplied by the change in the fluid velocity vector at the bend. For a 90 degree bend, this force is approximately given by the fluid density times the square of the average velocity, $\rho v^2$.

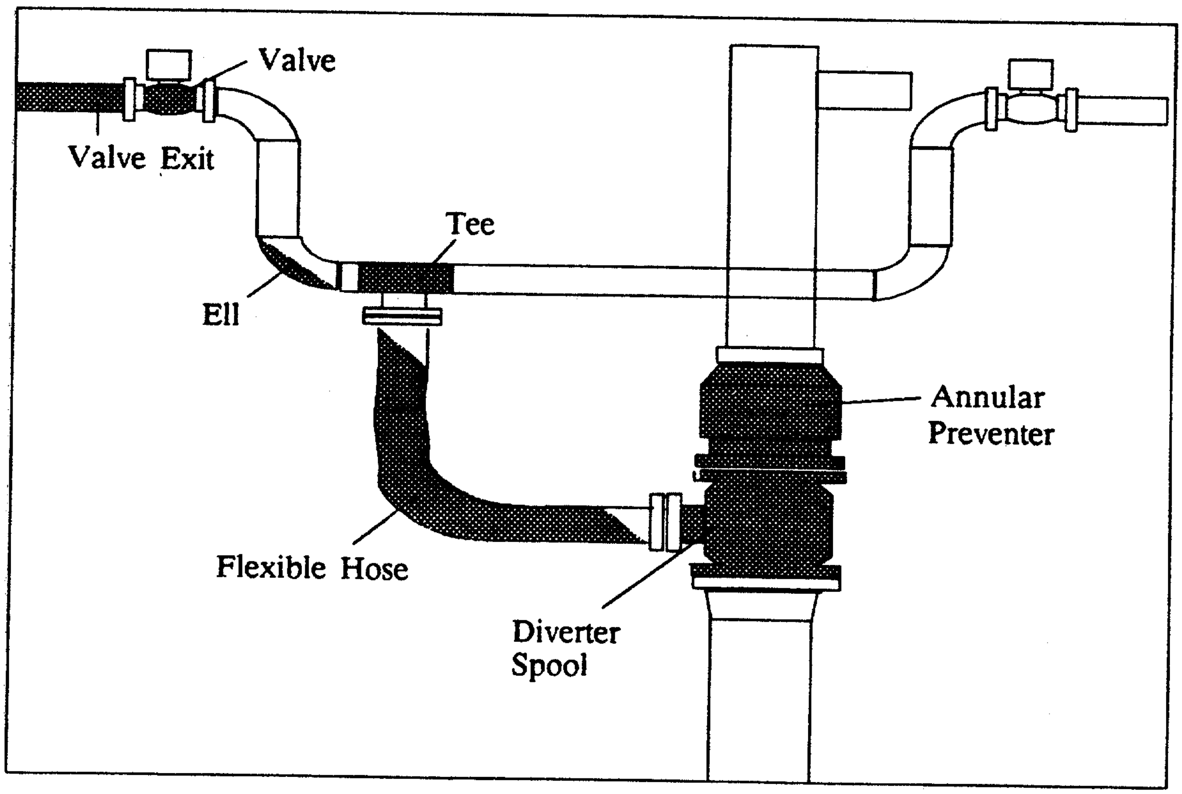


Figure 11 – Typical locations of erosive wear on diverter system for bottom supported rig. ( After Bourgoyne, 1989. )

*Rate of Erosion*

Information was collected on 31 wells that encountered shallow gas. Typical locations of erosion type failures are shown in **Figure 11** for a simplified diverter schematic. Problems tend to occur:

(1) at bends in the diverter line.
(2) at flexible hoses connecting the diverter to the wellhead.

(3) at valves or just downstream from valves.
(4) in the wellhead and diverter spool.

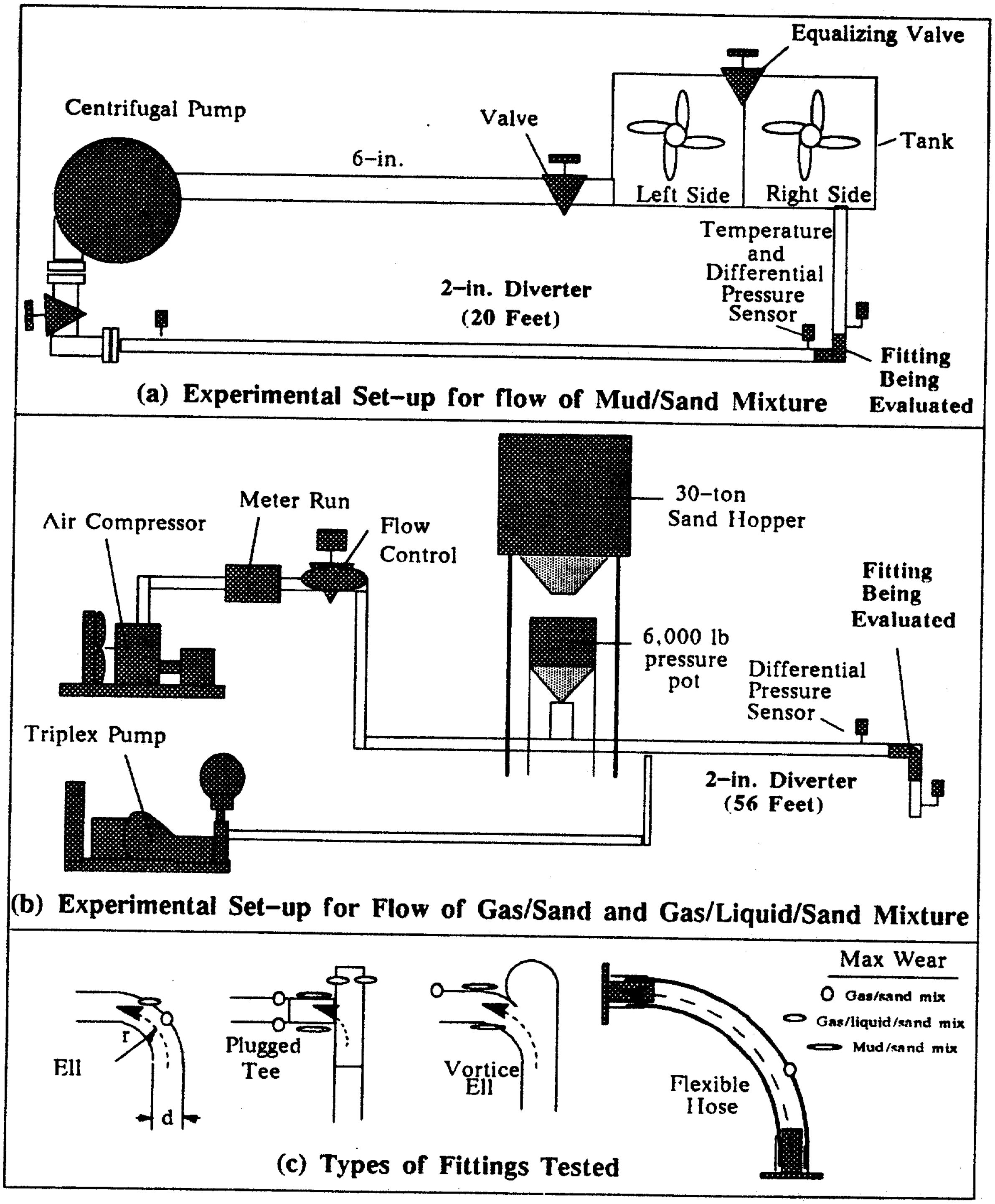


Figure 12 – Schematic of model diverter systems used in errosion study. ( After Bourgoyne, 1989. )

The severity of the erosion problems experienced was greatly affected by the quantity of sand produced by the well. When considerable sand was produced, diverter component failures started in the bends and valves and progressed back to the wellhead. The entire wellhead and annular preverter was cut from the well in an extreme case. For this well, sand piles of ten feet in height were reported on the rig floor after the well bridged.

Erosion can be caused by cavitation, impingement of liquids, or **impingement** of solid particles. Erosion by impingement of solid particles is the most **rapid** and is of primary concern for diverter operations. Previous erosion studies using flat plates, **[Finnie, 1967]**, **[Goodwin, 1969]**, **[Ives and Ruff, 1978]**, have shown that the total mass of material abraded from a solid surface is directly proportional to the total mass of abrasives striking the solid surface. Thus, the erosion resulting from abrasive particle impact is often expressed in terms of a *specific erosion factor, $F_e$, which is defined as the mass of steel removed per unit mass of abrasive.*

**Bourgoyne [1989]** used two experimental set–ups to measure the rate of erosion in various fittings. The first set–up (**Figure 12a**) was used for mud/sand slurries. Drilling mud flowed from the right side of a partitioned tank to a centrifugal pump, through 20 feet of 2–in. inside diameter pipe, through the fitting being evaluated, and then back into the tank. Flow rates were periodically checked by temporarily closing an equalizing line connecting the left and right sides of the tank. Sand concentration in the mud was also periodically checked by taking a sample from the tank.

The second set–up (**Figure 12b**) was used for gas/sand and gas/water/sand mixtures. Compressor supplied air flowed first through a flow control valve and 2–in. orifice meter. The flow control valve maintained a constant flow rate by means of a process control computer. Sand was added to the flow stream from a 6000–lb capacity sand blasting pressure pot through a metering valve. The weight of the pressure pot was continuously monitored, and the sand flow rate was determined from the rate of change of weight with time. Water or mud could be introduced downstream of the sand injection point. The mixture then flowed through 56 feet of 2–in. inside diameter line, through the fitting being evaluated, through a one–foot tail piece, and then exited to the atmosphere.

The fittings evaluated included steel Ells, plugged Tees, Vortice Ells, and rubber hoses (**Figure 12c**). Weight loss and wall thickness loss were periodically determined during the tests. Wall thickness measurements were made using an ultrasonic method. Thickness profiles were determined along both inside and outside radii of the bends. The location of the areas of maximum wear are shown in Figure 7.12c for the various fittings and fluid types studied. Data were collected to permit evaluation of sand rate, fluid velocity, fluid properties, and fitting type. The sand used in the experimental tests was No. 2 blasting sand.

The use of the specific erosion factor, Fe, for characterizing the effect of sand concentration on erosion in bends was evaluated using the data shown in **Figure 13**. Note that the wear rate was found to be directly proportional to the sand rate for the range of conditions studied. These sand rates were sufficient to result in sand concentrations of up to 0.12 percent. At high concentrations, significant decreases in the specific erosion factor would be expected due to interference **between** sand grains. However, the use of a constant value for the specific erosion factor appears acceptable for sand concentrations representative of diverter operating conditions.

Experiments were conducted to determine the effect of velocity on the rate of erosion for velocities of up to 220 m/s. The experimental results are shown in

**Figure 14**. The apparent slope of 2 includes the effect of increasing steel temperature with increasing flow velocity due to the sand particles impacting the wall of the fitting. At very high velocities, portions of the fittings were observed to smoke and begin to turn red due to very high temperature increases.

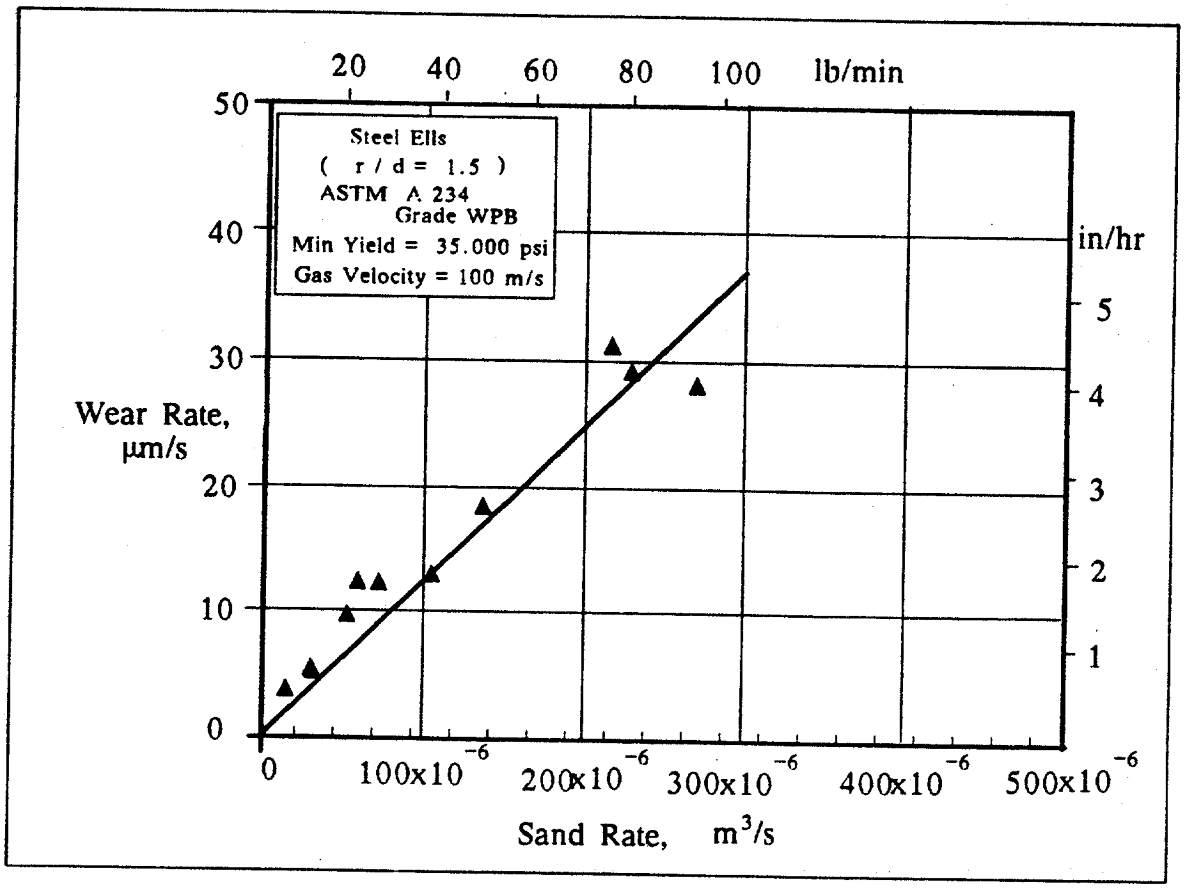


Figure 13 – Effect of sand concentration on rate of erosion at gas velocity of 100 m/s for ASTM a-234, Grade WPB ells with r/d=1.5 (Number 2 blasting sand) ( After Bourgoyne, 1989. )

Comparison of Specific Erosion Factors, $F_e$, obtained in similar fittings for mud carried abrasives and gas carried abrasives suggests that erosion rates are lower for mud by one to two orders of magnitude. The addition of small quantities of liquid to a gas/sand mixture was found to increase the specific erosion factor. The observed increase was more than would be expected due to the increase in gas velocity caused by the liquid hold-up. The presence of small quantities of liquid in the system appeared to increase the cutting efficiency of the sand. This was especially true in plugged Tees.

The higher erosion rates for gas is thought to occur because the transfer of momentum from the solids to the fluid is much less efficient. Thus, the solid particles strike the wall of a bend at a much greater angle in gas than in liquid. For ductile materials such as steel, the maximum rate of erosion occurs at an angle of impact with the eroding surface of about 20 degrees. For brittle materials, the maximum rate of erosion occurs at an angle of 90 degrees **[Ives and Ruff, 1978]**.

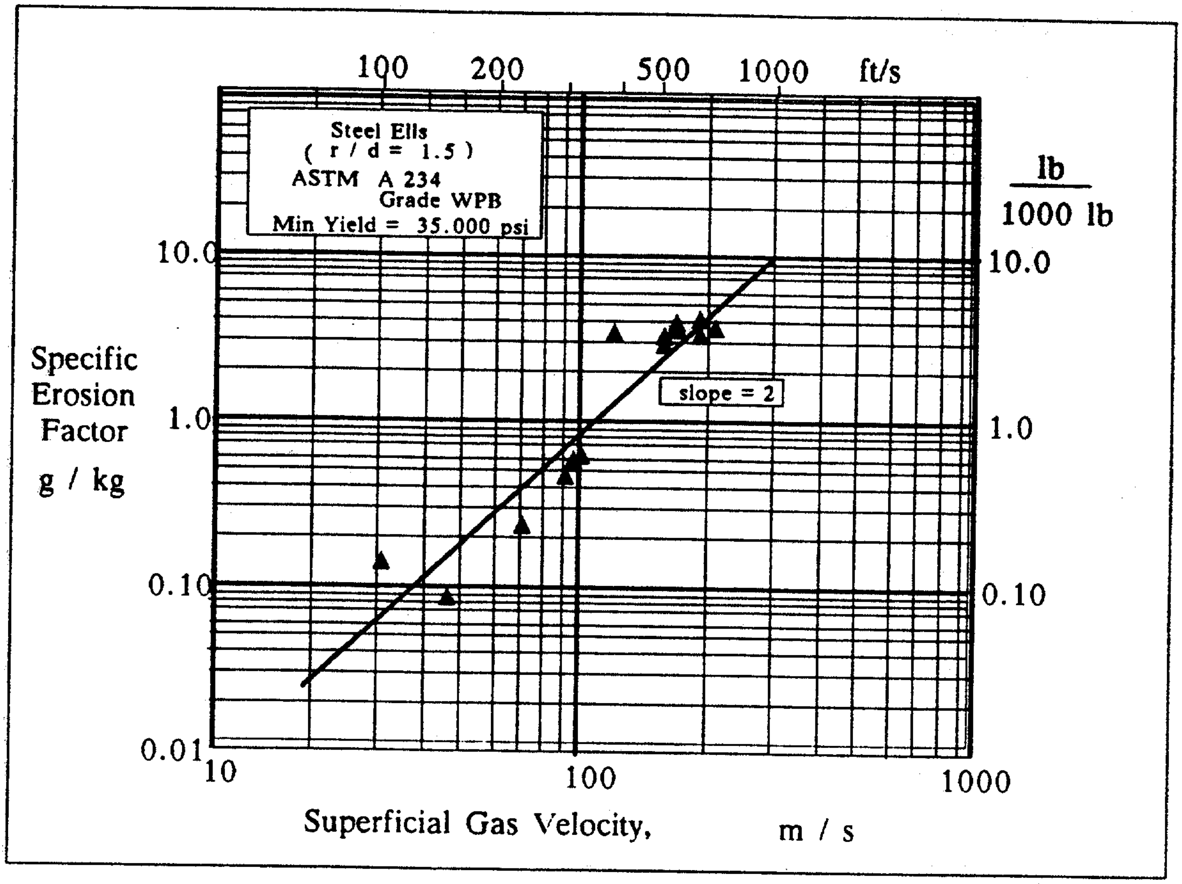


Figure 14 – Effect of gas velocity on rate of erosion for ASTM 234, Grade WPB ells with r/d=1.5 (Number 2 blasting sand) ( After Bourgoyne, 1989. )

Based on the experimental work performed **Bourgoyne [1989]** proposed the following equation in SI units for estimating the rate of loss in wall thickness, $h_w$, with time, t, in a diverter component of density, $\rho_s$, and cross sectional area , A, flowing abrasives having density, $\rho_a$, at a volumetric flow rate, $q_a$, and flowing gas or liquid at superficial velocity, $v_{sg}$ or $v_{sl}$, and volume fraction (holdup) $\lambda_g$ or $\lambda_l$:

*Gas Continuous Phase (Dry Gas or Mist Flow)*

$$\frac{dh_w}{dt} = F_e \frac{\rho_a}{\rho_s} \frac{q_a}{A} \left[ \frac{v_{sg}}{100\,\lambda_g} \right]^2 \tag{7.20}$$

*Liquid Continuous Phase*

$$\frac{dh_w}{dt} = F_e \frac{\rho_a}{\rho_s} \frac{q_a}{A} \left[ \frac{v_{sl}}{100\,\lambda_l} \right]^2 \tag{7.21}$$

Recommended values for specific erosion factor, $F_e$, are given in **Table 4**. The accuracy of the proposed calculation method was verified using the experimental data collected. The average error observed was 29 percent. This was felt to be an acceptable level of accuracy for diverter design considerations.

Table 4
Recommended Values of Specific Erosion Factor
Cast Steel is ASTM 216, Grade WBC and Seamless Steel is ASTM A234, Grade WPB

| Fitting Type | r / d | Material | Specific Erosion Factors ( g / kg ) Dry Gas Flow | Mist Flow | Liquid Flow |
|---|---|---|---|---|---|
| Ell | 1.5 | Cast Steel | 2.2 | 2.8 | 0.001 |
| | | Seamless Steel | 0.89 | 1.1 | |
| | 2.0 | Cast Steel | 2.0 | 2.4 | 0.001 |
| | | Seamless Steel | 0.79 | 0.93 | |
| | 2.5 | Cast Steel | 1.7 | 2.0 | 0.001 |
| | | Seamless Steel | 0.69 | 0.77 | |
| | 3.0 | Cast Steel | 1.5 | 1.65 | 0.0014 |
| | | Seamless Steel | 0.60 | 0.66 | |
| | 3.5 | Cast Steel | 1.2 | 1.32 | 0.0076 |
| | | Seamless Steel | 0.52 | 0.55 | |
| | 4.0 | Cast Steel | 0.9 | 1.0 | 0.01 |
| | | Seamless Steel | 0.45 | 0.49 | |
| | 4.5 | Cast Steel | 0.7 | 0.77 | 0.01 |
| | | Seamless Steel | 0.40 | 0.44 | |
| | 5.0 | Cast Steel | 0.5 | 0.55 | 0.01 |
| | | Seamless Steel | 0.35 | 0.38 | |
| Flexible Hose | 6.0 | Rubber | 1.00 | 1.22 | 0.02 |
| | 8.0 | | 0.40 | 0.45 | |
| | 10.0 | | 0.37 | 0.39 | |
| | 12.0 | | 0.33 | 0.35 | |
| | 15.0 | | 0.29 | 0.31 | |
| | 20.0 | | 0.25 | 0.28 | |
| Plugged Tee | — | Cast Steel | 0.026 | 0.064 | 0.0046 |
| | | Seamless Steel | 0.012 | 0.040 | 0.01 |
| Vortice Ell | 3.0 | Cast Steel | 0.0078* | | 0.0028 |

* Assumes Failure in Pipe Wall Downstream of Bend.

**Equations 20** and **21** were used to estimate the erosion life of various diverter components under a variety of assumed field conditions. Calculated erosion rates for various fittings and for a sand rate of 0.001 $m^3/s$ are shown in **Figure 15** as a function of superficial gas velocity. Note that erosion rates increase by two orders of magnitude as velocity increases from 30 m/s to the maximum (sonic) velocity of about 300 m/s. Note also, that for a given sand production rate, an order of magnitude decrease in erosion rate is predicted for changing from an Ell to a plugged Tee or Vortice Ell.

The use of **Eqn 20** for calculating the erosion life of various fittings for making a turn near the wellhead for the diverter system discussed in the previous example calculations is illustrated in **Table 5**. A design sand rate of 0.001 $m^3/s$ was used in these calculations. Note that for the 0.254–m (10–in.) system, the calculated time to failure is just seven minutes for a short radius ell. Use of a plugged tee would increase the estimated life to 8.9 hrs and use of a vortice ell would increase the estimated life to 13 hrs. The estimated life for a 0.152–m (6–in.) system would be about a third of that for the 0.254–m (10 in.) system.

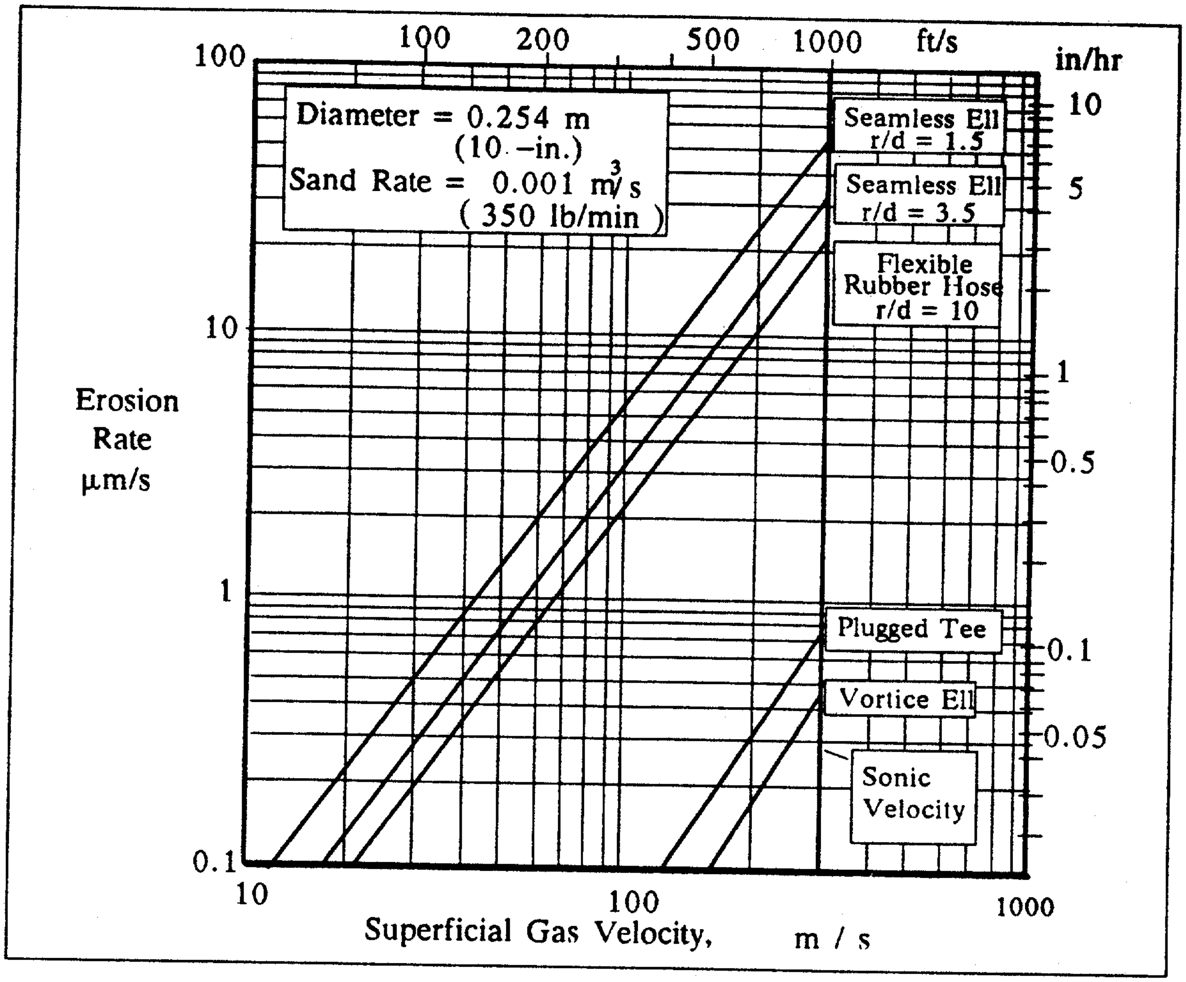


Figure 15 – Effect of fitting type on predicted erosion rate. ( After Bourgoyne, 1989. )

The calculations above illustrate the importance of avoiding bends in diverter systems. When a bend is required, a vortice ell or plugged tee should be used. When a plugged tee is used, metal targets in the dead–end branch can increase the erosion resistance to shallow gas flows containing significant quantities of water. However, field problems have been reported due to metal targets (lead fillings) breaking loose and moving downstream. Thus, targets should be designed as an integral part of the fitting.

*Plugging*

Solids in the drilling fluid tend to settle in the diverter components and can lead to valve malfunctions and plugging. To the extent possible, the diverter system is generally sloped towards its exit to promote draining and minimize the accumulation of solids in the system. In addition, provisions for flushing the system should be made. Clean–out connections with flushing jets should be placed upstream of all valves, bends, and local low spots.

Table 7.V
Comparison of erosion life near wellhead for various fittings used to make bend in 0.254-m (10-in.) diverter system and 0.154-m (6-in.) diverter system.

| Parameter | Units | 0.152-m (6-in.) Diameter | | 0.254-m (10-in.) Diameter | |
|---|---|---|---|---|---|
| Wall Thickness | m<br>in. | 0.0071<br>0.28 | | 0.00927<br>0.365 | |
| Flowrate at S.C. | $m^3/s$<br>MMScf/D | 40.8<br>124 | | 43.3<br>132 | |
| Pressure at Fitting | Pa<br>psi | 1,485,000<br>215 | | 488,000<br>71 | |
| Temperature at Fitting | °C<br>°F | 38<br>100 | | 38<br>100 | |
| Flowrate at Fitting | $m^3/s$<br>MMScf/D | 3.0<br>9.2 | | 9.7<br>29.5 | |
| Velocity at Fitting | m/s<br>f/s | 165<br>542 | | 191<br>628 | |
| Gas Volume Fraction | | 0.9997 | | 0.9999 | |
| Erosion Rates | | | | | |
| Ell-r/d=1.5<br>$F_e$ =0.00089 | m/s<br>in./hr | $4.5 \times 10^{-5}$<br>6.4 | (3 min) | $2.2 \times 10^{-5}$<br>3.1 | (7 min) |
| Flexible Hose<br>$F_e$ =0.00033 | m/s<br>in./hr | $1.7 \times 10^{-5}$<br>2.4 | (7 min) | $8.0 \times 10^{-6}$<br>1.1 | (20 min) |
| Plugged Tee<br>$F_e$ =0.000012 | m/s<br>in./hr | $6.1 \times 10^{-7}$<br>0.087 | (3.2 hr) | $2.9 \times 10^{-7}$<br>0.041 | (8.9 hr) |
| Vortice Ell<br>$F_e$ =0.000008 | m/s<br>in./hr | $4.0 \times 10^{-7}$<br>0.058 | (4.8 hr) | $1.9 \times 10^{-7}$<br>0.028 | (13 hr) |

*Control System*

Control of the diverter vent lines should be achieved by means of valves that can be fully opened to minimize erosion and pressure losses. The diverter control system generally involves pneumatic or hydraulic valve operators and can be operated from remote panels located with the blowout-preventer control panels. It is often advantageous to integrate the diverter control system with the blowout preventer control system. Standards regarding the accumulator unit which stores the pressurized control fluid needed to operate the valves, should be similar to those adopted for the blowout preverter system. A non-flammable, low-freezing-point power fluid should be used in the hydraulic units. The controls should be designed so that the well cannot be closed with the diverter system, i.e. the valves to the vent line should automatically open before the annular sealing device is closed. When multiple vent lines are needed to insure downwind diversion, the currently selected vent valve should open before the other vent valve is closed. Specially designed integral sequencing diverter components have recently become available that provide the annular sealing system and vent line valve in a single unit **[Roche, 1986]**.

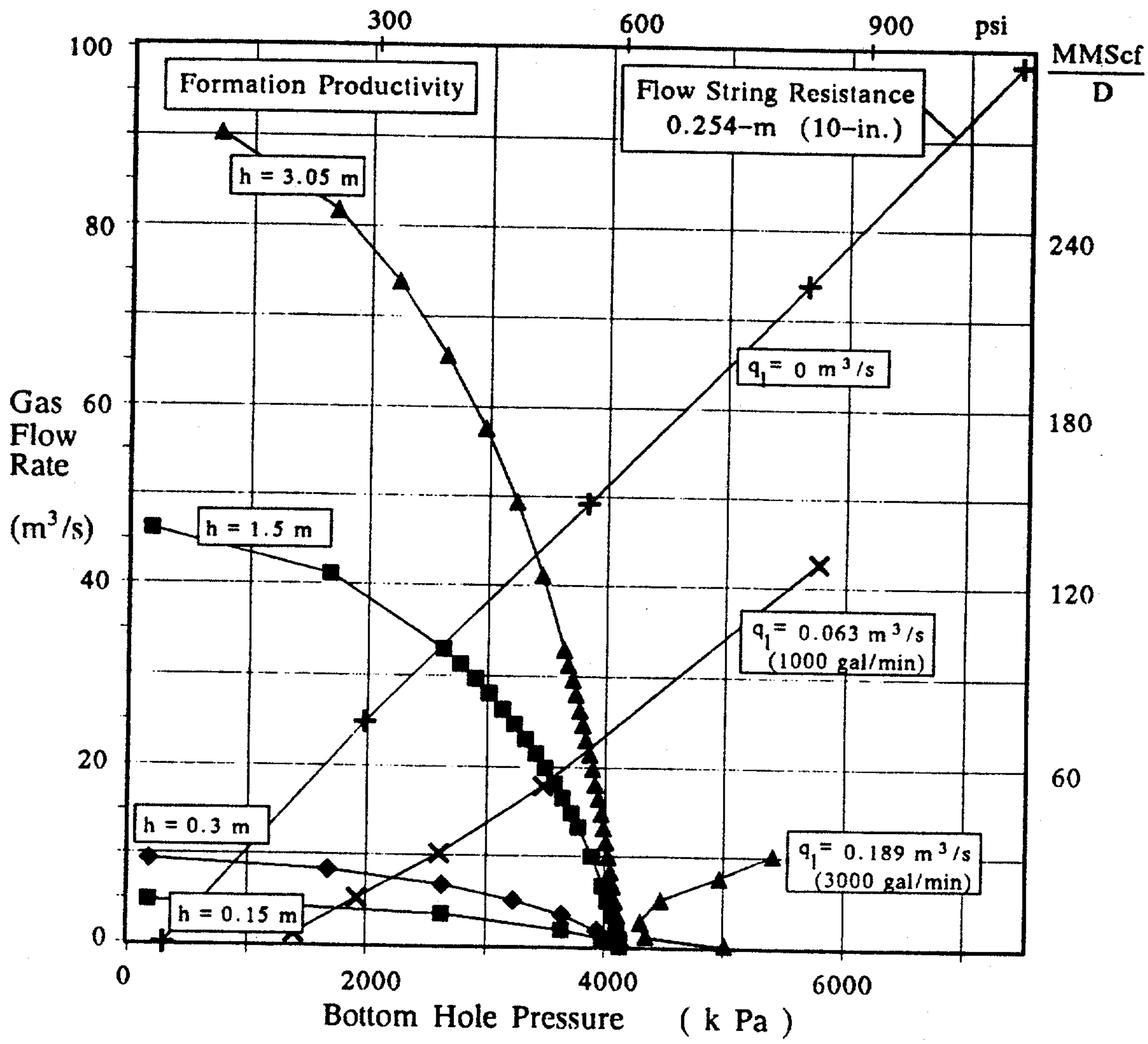


Figure 16 – Pseudo-steady-state systems analysis plot for dynamic well control attempt using available rig pumps.

*Design Considerations for Dynamic Kill*

Some operators use a contingency plan which calls for a "dynamic" well control procedure to be attempted as soon as the well is placed on a diverter. The dynamic well control procedure has been described in detail by **Blount and Soeiinah [1981]**. With this method, high-circulating rates are used to increase annular frictional pressure losses sufficiently to cause the bottom-hole pressure to be raised above the formation pressure. Some operators maintain a volume of weighted drilling fluid on location for use in an immediate attempt at a dynamic kill. Other operators plan the use of seawater after the available mud volume has been exhausted. The success of the dynamic well control method is governed primarily by the flow rate and pressure limitations of the available rig pumps and the effective thickness of the gas formation penetrated by the bit before the gas flow is detected. Data that was collected on 28 shallow gas flows occurring in the Gulf of Mexico indicates that in two cases the flow was successfully stopped using a dynamic kill procedure.

When a dynamic well control procedure is included in the shallow gas contingency plan, the diverter design load should be based on the well conditions that will result with the rig pumps operating at the maximum available flow rate. The basic calculation procedure remains unchanged, except that the liquid pumped is added to the formation gas being produced on bottom. Shown in **Figure 16** is a systems analysis plot for a dynamic kill attempt using seawater at a maximum pump rate of 0.063 $m^3$ /s (1000 gal/min). Formation productivity curves are shown for a range of effective formation thickness value from 0.15m to 3.05m (0.5 ft to 10 ft). Flow-string resistance curves are shown for both a non-pumping case and for a dynamic kill attempt at the maximum available pump rate. Note that for the maximum effective formation thickness value considered, the dynamic well control method would reduce the equilibrium gas flow rate from 43 $m^3$ /s to 22 $m^3$ /s (132 MMScf/D to 67 MMScf/D), but would not bring the well under control. Note also that control is not predicted for any of the effective formation thickness values considered. These calculations suggest that the dynamic well control method will be successful only for very thin formations or low-permeability formations.

Using the methods previously presented, it can be shown that the pressure at the casing seat during the dynamic kill attempt would increase slightly to 525,000 Pa (76 psi). Since the fracture pressure is 1,467,000 Pa (214 psi), the 0.254-m (10-in.) diverter system would be adequate to permit the dynamic well control method to be tried. The peak pressure observed when the gas first reaches the surface would be reduced from 1,436,000 Pa to 1,138,000 Pa (208 psi to 165 psi). The velocity at a bend near the wellhead would be reduced from 191 m/s to 131 m/s resulting in about a 40 percent reduction in the erosion rate at this location.

Even when the dynamic well control method cannot be successfully employed using the available rig equipment, there is a high probability that control of the well can be regained through borehole collapse or reservoir depletion. In 25 of 28 shallow gas flow events that occurred in the Gulf of Mexico ( 90% ), the well plugged due to borehole collapse. In 14 cases ( 50% ), flow stopped within a one day period. In 22 cases ( 79% ), flow stopped within a one week period. However, in one case, two relief wells had to be drilled before the well could be brought under control with auxillary pumping equipment.

**Koederitz, Beck, Langlinais, and Bourgoyne [1987]** developed a computer program for determining the flow rate and pressure requirements required to bring a shallow gas flow under control using the dynamic well control method. The program can be used to evaluate the requirements for regaining control either using the existing wellbore, or using one or more additional relief wells. The program is based on the systems analysis approach illustrated in the previous example, except that the analysis is repeated at successively higher pumping rates until well control is indicated by the lack of an intersection between the flow-string resistance curve and the formation inflow-performance curve. The flow-string resistance curve at the minimum pump rate required for well control for the previous example is also shown in **Figure 16**. Note that a pump rate of 0.189 $m^3$ /s (3,000 gal/min) would be required. At least one relief well would be needed to achieve this rate without exceeding a maximum pump pressure of 15,000 psi.

The program developed by **Koederitz, Beck, Langlinais, and Bourgoyne [1987]** also determines the maximum pressure experienced at every point in the borehole as the pumping rate is increased up to the value required to bring the well under control. It was found that the maximum pressure at a given point in the borehole does not necessarily occur at the maximum liquid rate. Ideally, the diverter design would permit any pumping rate up to the kill rate to be maintained without exceeding the fracture pressure. Shown in **Figure 17** is a comparison of the fracture and borehole pressures as a function of pumping rate for the previous example. The calculations indicate that the 0.254-m (10-in.) diverter system would achieve this design objective.

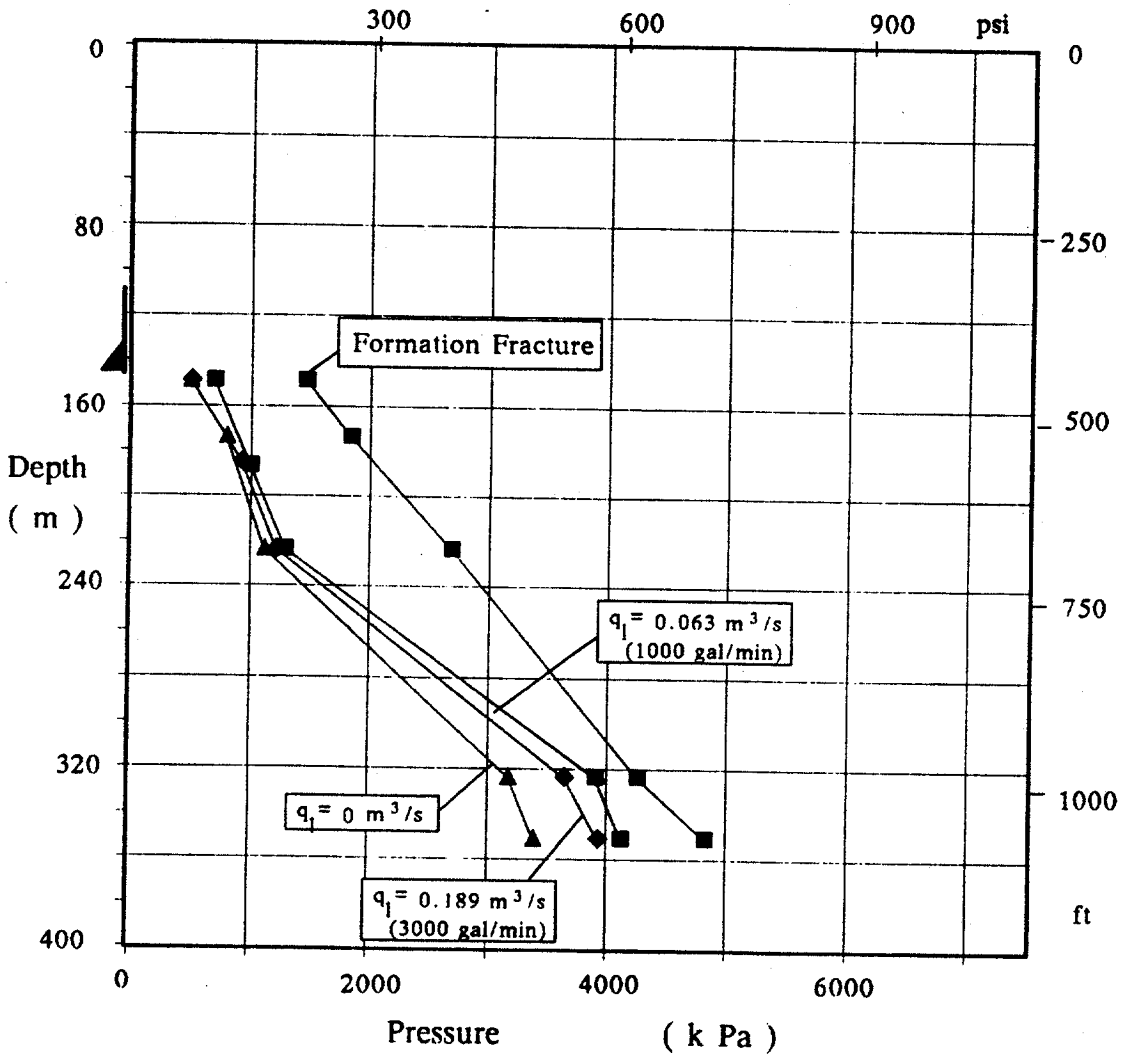


Figure 17 – Pseudo-steady-state systems analysis plot for dynamic well control attempt using available rig pumps.

## Diverter Operation

The infrequent use of the diverter system increases the need for scheduled system maintenance and personnel training activities. Since a shallow gas flow can surface in a matter of minutes, there will be little time for coummunicating instructions to the rig crew after the flow is detected. Calculation results used to verify the adequacy of the diverter system for the anticipated drilling plan are also useful for personnel training. Each member of the rig crew should throughly understand the contingency plans that will be used in the event of a shallow gas flow and the action required from them when executing these plans. They should also understand the purpose and importance of the activities directed towards system maintenance. A properly designed system will be of no use if it is not properly maintained.

In operation, the diverter system should be used primarily to provide time for an orderly rig abandonment. If the shallow gas flow is detected before the bit has opened a significant thickness of the gas bearing formation, or if the formation permeability is low, use of the dynamic well control method may be successful. However, the diverter exit should be carefully monitored to detect when the flow velocity begins to approach sonic velocity and to detect sand production. A transducer at the diverter exit that could detect the onset of sonic flow, and estimate gas rates would be very useful. A sand probe that could detect significant levels of sand production is also needed. A novel diverter exit monitor is under development as a result of the research completed at LSU.

### Special Considerations for Floating Drilling Vessels

When drilling from a floating vessel, the operator has more options available for handling a shallow gas flow. The vessel is not supported from bottom, so the danger of loosing the vessel to a crater is no longer present. Various options that are available are illustrated in **Figure 18**. Each of these options have different advantages and disadvantages, and their use must be based on the drilling conditions anticipated.

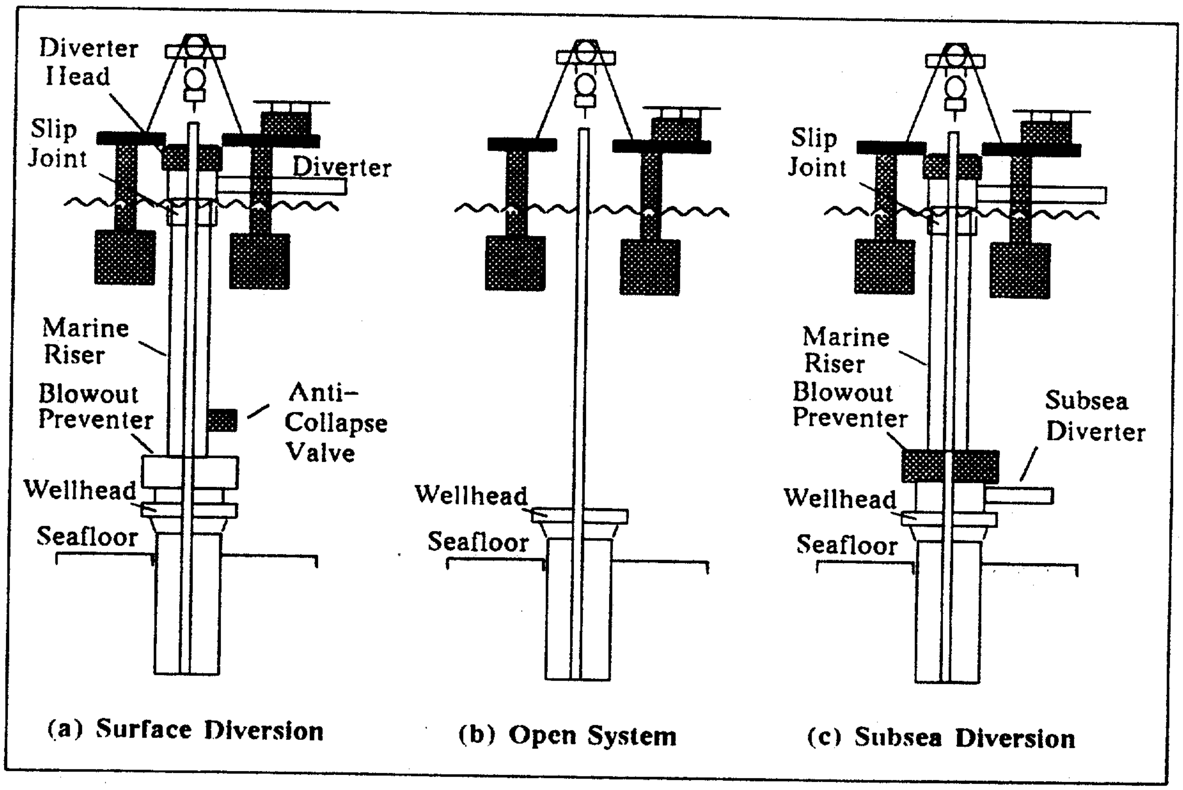


Figure 18 – Various methods for handling shallow gas flows on floating **drilling vessels**

The option illustrated in **Figure 18a** is similar to the approach used with a bottom supported vessel. During drilling operations, the drilling fluid is returned to the surface through the marine riser. If a shallow gas flow is encountered, an annular sealing device or diverter head located at the top of the marine riser is closed, and the gas flow is vented through a conventional diverter system attached to the marine riser below the sealing assembly. An annular blowout preverter with the associated choke and kill lines may also be deployed below the marine riser.

The use of a surface diverter system (**Figure 18a**) has the advantage of maintaining a closed drilling fluid system in which fluid properties can be controlled. When formation fracture pressures permit, better control of the borehole pressures can be maintained through selection of an appropriate drilling fluid density. This increases the ability to prevent a shallow gas flow. When the formation fracture pressure is low, it may not be possible to bring drilling fluid back to the vessel without the aid of booster lines used to gas lift the marine riser. Subsea valves may also be used to periodically release dense drilling fluid that has become loaded with drilled cuttings at the seafloor. Use of the surface diverter system has the disadvantage of bringing the gas on board the vessel, perhaps creating a need to abandon the vessel for personnel safety. An abandoned floating vessel may not be able to maintain its station over the subsea wellhead. Also, the slip joint used to permit motion of the floating vessel relative to the wellhead is difficult to design for maintaining a pressure seal and introduces a weak link in the system. The marine riser must also be designed to withstand the external pressure of the seawater while containing only gas. Several cases of riser collapse have occurred which indicates an elastic collapse mode of failure. This failure mode is controlled by the diameter to wall thickness ratio, and is independent of the yield strength of the steel used **[Erb, Ma, and Stockinger, 1983]**.

The pressure–integrity problem of the slip joint (**Figure 18a**) can be eliminated through use of a newly available annular sealing unit that can be placed below the slip joint. Outlets below the sealing unit are attached to the surface vent lines by means of flexible hoses. **[Hall, Roche and Boulet, 1986]**.

When it is not feasible to design the marine riser to withstand the full collapse loading of the sea at the water depth of interest, an anti–collapse valve can be used in the marine riser (**Figure 18a**). This valve will automatically open when the internal pressure in the marine riser falls too low, admitting seawater to the marine riser. The systems analysis procedure described previously can be used to determine the flow rate at which seawater will enter. This is accomplished by modifying the procedure used to calculate the flow string resistance at a given gas flow rate. The flow string resistance must be computed for various assumed seawater flow rates through the anti–collapse valve. The correct flow string resistance curve is then selected based on a knowledge that the pressure in the marine riser at the valve must be equal to the pressure in the ocean at that depth, less any pressure drop across the valve due to the flow of seawater.

Another option that can be used with the equipment arrangement shown in **Figure 18a** is to close the annular blowout preventer at the seafloor and accept the possibility of seafloor fracturing. If gas begins surfacing near the vessel, procedures for detaching from the wellhead and moving the vessel can be implimented. In deep water, the gas may be carried a considerable distance from the vessel. In addition, much of the gas may go into solution in the seawater. The solubility of natural gas in seawater increases significantly with increasing pressure and decreasing temperature **[Dodson and Standing, 1944]**.

The option illustrated in **Figure 18b** is the use of an open system in which the drilling fluid and cuttings are discharged at the seafloor. No marine riser is deployed and seawater is generally used for the drilling fluid. In the event of a shallow gas flow, gas is discharged through the open wellhead at the seafloor. Returns at the seafloor are generally monitored with a subsea camera. The pressure at the wellhead is maintained at the hydrostatic pressure of the ocean for the given water depth, causing borehole pressures to be maintained at a higher value than for a surface diversion. This results in a lower gas rate but may also reduce the tendency for the well to plug by borehole collapse, especially in very deep water. This option is best suited for areas where the formation pore pressures and fracture pressures are known to be low. All of the problems of returning the drilling fluid to the surface vessel without causing formation fracture are avoided. The major disadvantages of this approach is an inability to increase the drilling fluid density to minimize the chance of a shallow gas flow from an abnormally pressured formation, and the possibility of a gas boil near the vessel. However, if gas begins surfacing near the vessel, the vessel can be moved from above the wellhead.

The option illustrated in **Figure 18c** involves the use of a subsea diverter system between the wellhead and the marine riser. This system has the advantages of a closed drilling fluid system in which the drilling fluid density can be controlled, but yet does not require that the gas flow be brought on board. The diverter is short, so the problems associated with the possibility of gas surfacing near the vessel remain. In addition, the time required to leave the location is greater than that of an open system.

**Recommendations**

As a result of the research conducted, the following recommendations are made:

1. Seismic surveys should be made at proposed offshore wildcat-well locations and the data processed for shows of gas and for abnormal pressure detection.

2. Maximum safe drilling rates should be estimated for the shallow portion of a well in which gas-cut mud could increase the risk of a shallow gas flow.

3. A systems analysis design procedure should be employed for proposed wildcat wells to verify the adequacy of the planned casing program for the available diverter system. The systems analysis should consider the possibility of sonic flow velocity at the diverter exit and at restrictions in the flow path.

4. The working pressure of a diverter system should be based on pressure peaks that could be expected during the unloading of the drilling fluid from the well.

5. Bends in diverter vent lines should be avoided whenever possible. When bends are required, a plugged tee or vortice ell should be used.

6. Dynamic well control methods have been successfully used to control some shallow gas flows with available rig pumps. However, a diverter exit monitor should be developed which will detect sonic flow, significant levels of sand production, and provide appropriate warning when these conditions are detected.

7. When shallow gas flows are severe, the diverter system on a bottom supported drilling vessel should be used primarily to provide time for a orderly rig abandonment.

**Acknowledgement**

The research which formed the basis for this report was supported by the U.S. Minerals Management Service and by unrestricted grants from ARCO, Chevron, and Conoco. Equipment grants were provided by Daniel, Dresser Industries, Foxboro, Hydril, and Rosemount Instruments.

**References**

**Beck,F.E., Langlinais, J.P., and Bourgoyne, A.T.**: "Experimental and Theoretical Considerations for Diverter Evaluation and Design," SPE 15111, Carfonia Regional Meeting of SPE, Oakland, California, April 3–6, **1986**.

**Beck,F.E., Langlinais, J.P., and Bourgoyne, A.T.**: "An Analysis of the Design Loads Placed on a Well by a Diverter System," SPE/IADC 16129, Drilling Conference, New Orleans, La., March, **1987**.

**Blount, E.M. and Soeiinah, E.**: "Dynamic Kill: Controlling Wells in a New Way," World Oil, pp 109–126, October, **1981**.

**Bourgoyne, A.T., Hise, B.R., Holden,W.R., and Sullins, R.S.**: "Well Control Procedures for Deepwater Drilling – Part 2: Control of Shallow Kicks," Ocean Resources Engineering, pp 8–18, October, **1978**.

**Bourgoyne, A.T.,Millheim, K.K., Chenevert, M.E., and Young, F.S.**: "*Applied Drilling Engineering*," SPE Textbook Series, Vol.2, Dallas, Texas, pp 252–285, **1986**.

**Bourgoyne, A.T.**: "Experimental Study of Erosion in Diverter Systems Due to Sand Production," SPE/IADC 18716, Drilling Conference, New Orleans, Louisiana, pp 807–816, **1989**.

**Brown, K.E.,and Beggs, H.D.**: "*The Technology of Artificial Lift – Volume I: Methods*", Penn Well Books, Tulsa, Oklahoma, **1977**.

**Constant, W.D. and Bourgoyne, A.T.**: "Fracture–Gradient Prediction for Offshore Wells," SPE Drilling Engineering, pp 136–140, June, **1988**.

**Clark, A.R. and Perkins, T.K.**: "Wellbore and Near Surface Hydraulics of a Blown–out Oil Well," SPE 9257, Annual Fall Meeting of SPE, Dallas, Texas, 6 pp, September 21–24, **1980**.

**Craft, B.C. and Hawkins, M.F.**: "*Applied Petroleum Reservoir Engineering*," Prentice Hall, Inc., Englewood Cliffs, New Jersey, **1959**.

**Crouch, E.C., and Pack, K.J.**:" 'Systems Analysis' Use for the Design and Evaluation of High Rate Gas Wells," SPE 9422, Annual Fall Meeting of SPE, Dallas, Texas, 4 pp, September 21–24, **1980**.

**Dodson, C.R. and Standing, M.B.**: "Pressure–Volume–Temperature and Solubility Relations for Natural Gas–Water Mixtures," Drilling and Production Practice, API, p.173, **1944**.

**Erb, P.R., Ma, T.C., and Stockinger, M.P.**: "Riser Collapse – A Unique

Problem in Deep-Water Drilling," IADC/SPE 11394, Drilling Conference, New Orleans, Louisiana, pp 307-312, February 20-23, **1983**.

**Finnie, I** : "Erosion of Surfaces by Solid Particles," Wear, v 3, pp 87-103, **1960**.

**Forchheimer, P.**: "Wasserbewegung durch Boden," Zeitz, ver dutch, Ing. v 45 p 1731, **1901**.

**Goodwin, J.E., Sage, W., and Tilly, G.P.**: Proceedings of the Institute of Mechanical Engineers, v 184, pp 279-292, **1979**.

**Hall, J.G., Roche, J, and Boulet, C.H.**: "Means for Handling Gas Influx in Marine Risers," SPE/IADC 14739, Drilling Conference, pp 173-176, New Orleans, Louisiana, February, **1986**.

**Ives, L.K., and Ruff, A.W.**: Wear, V46, pp 149-162, **1978**.

**Johnson, T.W. and Taliaferro, D.B.**: "Flow of Air and Natural Gas Through Porous Media," Technical Paper 592, USBM, **1938**.

**Prior, D.B., Doyle, E.H., and Kaluza, M.J.**: "Evidence for Sediment Eruption on Deep Sea Floor, Gulf of Mexico," Science, Vol. 243, pp 517-519, January 27, 1989.

**Koederitz, W.L., Beck, F.E., Langlinais, J.P., and Bourgoyne, A.T.**: "Methods for Determining the Feasibility of Dynamic Kills for Shallow Gas Flows," SPE 16691, Annual Fall Meeting of SPE, Dallas, Tx. , Sept., **1987**.

**Moody, L.F.**: "Friction Factors for Pipe Flow," Trans. ASME, V 66, p 671, **1944**.

**Roche, J.**: "Diverter Improvements Help Handle Shallow Gas Kicks Safely," Oil and Gas Journal, February 10, **1986**.

**Ross, N.C.J.**: "An Analysis of Critical Simultaneous Gas-liquid Flow through a Restriction and its Application to Flow Metering," Applied Science Res. Vol 9, p 374, **1960**.

**Santos, O. and Bourgoyne, A.T.**: "Estimation of Peak Pressures Occurring when Diverting Shallow Gas," SPE 19559, Annual Fall Meeting of SPE, San Antonio, Texas, October 7-8, **1989**.

**Tolle, G.C., and Greenwood, D.R.**: "Design of Fittings to Reduce Wear Caused by Sand Erosion", American Petroleum Institute OSAPR Project No. 6, Texas A&M, College Station, Tx. May, **1977**.

**Wallis, G.B.**: "*One Dimensional Two-Phase Flow*," McGraw-Hill Book Co., Inc., New York, **1969**.

## NOMENCLATURE

| | | |
|---|---|---|
| A | – | Cross sectional area, m |
| c | – | Compressibility, $Pa^{-1}$ |
| d | – | Diameter. |
| k | – | Ratio of heat capacity at constant pressure to heat capacity at constant volume. |
| $f$ | – | Moody friction factor. |
| F | – | Specific Erosion Factor, kg/kg |
| h | – | Thickness, m. |
| k | – | Permeability, $m.^2$ |
| M | – | Molecular weight. |
| n | – | Polytropic expansion coefficient. |
| p | – | Pressure, Pa. |
| q | – | Volumetric flow rate, $m^3/s$. |
| r | – | Radius. |
| R | – | Universal gas constant. |
| t | – | Time, s |
| T | – | Temperature, °K. |
| v | – | Velocity, m/s. |
| z | – | Gas deviation factor. |
| $\beta$ | – | Velocity Coefficient, $m.^{-1}$ |
| $\epsilon$ | – | Roughness, m |
| $\lambda$ | – | Fractional volume or holdup. |
| $\mu$ | – | Viscosity, Pa s. |
| $\theta$ | – | Vertical deviation angle, rad. |
| $\rho$ | – | Density, $kg/m.^3$ |
| $\sigma$ | – | Stress. |
| $\chi$ | – | Weight fraction or quality. |

Subscripts

| | | |
|---|---|---|
| 1,2 | – | Reference depths of casing seat and bit. |
| a | – | Abrasive. |
| bh | – | Bottom-hole. |
| e | – | Effective, Also external reservoir limit. |
| f | – | Formation, also fracture. |
| g | – | Gas. |
| l | – | Liquid. |
| ls | – | Liquid/solid mixture. |
| ob | – | Overburden. |
| p | – | At constant pressure; Also pore; Also thickness penetrated. |
| s | – | Solid; Also steel; Also sediments. |
| sc | – | Standard conditions. |
| sg | – | Superficial gas flux. |
| sl | – | Superficial liquid flux. |
| sw | – | Seawater. |
| v | – | At constant volume. |
| w | – | Wall, also wellbore. |